Please cite this article in press as: Casebolt et al., Pulse check: Potential opportunities in pulsed electrochemical CO_2 reduction, Joule (2021), https://doi.org/10.1016/j.joule.2021.05.014

Joule

CellPress

Review

Pulse check: Potential opportunities in pulsed electrochemical CO_2 reduction

Q1 Rileigh Casebolt,[1] Kelsey Levine,[1] Jin Suntivich,[2] and Tobias Hanrath[1]

SUMMARY

Developing affordable, robust, and selective CO2 electroreduction technologies is crucial to address concerns about rising CO2 emissions. Pulsed potential electrochemical CO2 reduction (p-eCO2R) has emerged as a simple and responsive knob to increase electrolyzer durability and improve product selectivity. In this review, we summarize the recent findings of p-eCO2R on copper electrodes as a function of applied potential and pulse duration. We discuss how pulse methods present scientific and technological opportunities for electrochemical technologies beyond p-eCO2R, in particular, ones involving competing reactions or electrode deactivation.

Q4 Q3 Q2 INTRODUCTION

Electrochemistry is pervasive in most aspects of our lives—from redox reactions that sustain our bodies, industrial productions of chemicals and materials, and biochemical sensors for healthcare monitoring, to batteries for personal electronics and electric vehicles.[1–3] The profound technological and industrial impacts of electrochemical processes derive from their scalability and our ability to control the electrochemical reactions with a simple electrochemical-potential knob. In the face of growing concerns about anthropogenic CO_2 emissions and related climate change, scientists and engineers are looking to electrochemistry as an approach to address the rising atmospheric CO_2 levels. Developing electrochemical routes to valorize CO_2, a solution whereby renewable energy can be used to close the carbon cycle, thus transforming CO_2 into valuable molecules is within the realm of possibility.[4–6] Crucial to bringing this vision to fruition is the development of catalysts and electrochemical systems that can stably reduce CO_2 to value-added molecules at industrially relevant conditions with reasonable durability, lifetime, and product selectivity.[7]

Recent years have borne witness to exciting experimental and computational scientific achievements, which have significantly improved our understanding and design of electrodes, electrolytes, and electrolyzers for CO_2 electrolysis. Initially, efforts in the community have focused on improving the electrochemical rates (activities), reaction selectivity, and the overpotential at which CO_2 reduction products are formed by separately engineering the electrode, electrolyte, or balance of the system.[5] However, it is becoming clear that the processes in these different components are connected. We point the readers to several excellent reviews about the role of catalyst, electrolyte, and cell design in the electrochemical CO_2 reduction (eCO_2R) reaction.[5,6,8–19] From a system-level perspective, it is important to consider not only the energy required to reduce CO_2 in the first place but also to address the downstream energy requirement of separating the resulting multitude of products. A recent technoeconomic analysis concluded that for a system to operate at a favorable energy return on energy investment, the energy requirements of separation

Context & scale

Pulsing electrochemical variables (e.g., voltage/current modulation) represents a simple experimental "knob" to influence product selectivity and electrode longevity in electrochemical CO_2 reduction (eCO_2R). By tuning the interfacial factors (e.g., hydrodynamics, ad/desorption, surface reconstruction, catalyst oxidation, etc.) and their variations with pulse profile (e.g., duration and potential), the application of pulsed potential can tip the balance between transient physicochemical processes at electrode/electrolyte interfaces, the result of which can impact the eCO_2R outcome.

Pulsed eCO_2R (p-eCO_2R) has broad implications spanning multiple length and timescales. At atomic scales, the pulsed potential influences the dynamic restructuring of surfaces and distribution of surface-adsorbed species; at millisecond-to-second timescales, the pulsed potential impacts the profiles of interfacial water, ions, and intermediates within the electrical double layer (EDL). Finally, at minute-to-hour timescales, the pulsed potential can mitigate surface deactivation to ensure electrode durability. Using pulsing to control the reaction microenvironment is a cost-effective "plug-and-play" approach to impact reaction durability and selectivity, bringing

Please cite this article in press as: Casebolt et al., Pulse check: Potential opportunities in pulsed electrochemical CO_2 reduction, Joule (2021), https://doi.org/10.1016/j.joule.2021.05.014

should be less than half of the product enthalpy of combustion.[20] Using the separations costs listed in Greenblatt et al.,[20] the isolation of ethanol from an aqueous input stream requires 4.7 MJ/kg, which is 25% of the total energy required for converting CO_2 into ethanol (Section S2); this percentage increases drastically for less-concentrated input streams. Considering the high separation costs and necessary improvements in reaction selectivity, in this review we focus on selectivity, rather than activity.[21,22]

Although copper (Cu) electrodes are unique by virtue of the fact that they are the only monometallic electrocatalysts that yield high-value C_{2+} products at reasonable rates, the Cu-catalyzed reaction is not very selective.[5] Cu's unique ability to promote C–C coupling comes from its favorable binding energies to eCO_2R intermediates, specifically its binding energy to CO, a common eCO_2R intermediate.[23,24] The CO binding on Cu is neither too weak that it desorbs from the surface before coupling, nor too strong that it desorbs too slowly and blocks active sites.[25] As a result, Cu can sustain a significant coverage of adsorbed CO on the surface, which can increase the probability of C_{2+} product formation.[26] In addition to this paradigm of optimal CO binding energy, there is also increasing evidence that other adsorption energies contribute to resulting selectivity (including *H, *COOH, and $*CH_3O$).[24] However, the high activity to form C_{2+} products on Cu comes at a cost of low product selectivity—up to 16 different products have been reported.[27] Instead of accepting this trade-off between producing multi-carbon products and paying significant energy costs for downstream separation processes, we endeavor to improve the product selectivity from the start. As detailed below, the application of a pulsed potential electrochemical CO_2 reduction (p-eCO_2R) has emerged as an intriguing experimental knob to tune the product selectivity.

A holistic approach to bring eCO_2R to technological fruition must also consider the longevity of the electrolyzer. Conventional Cu-based electrolysis cells commonly used in academic studies suffer from short operating lifetimes, which presents a significant barrier to translate these advances from lab to market.[28,29] Starting in the 1990s, electrochemical approaches briefly reversing the applied voltage (i.e., anodic treatments) were explored to recover catalyst activity. Seminal work by Shiratsuchi et al. found that periodically interrupting the electrolysis with short anodic pulses prolongs the lifetime of the copper catalyst and alters the product selectivity.[30] Whereas the conventional constant-potential cells typically lasted only a few hours before experiencing a loss of catalytic activity and a corresponding shift in product selectivity toward the undesirable hydrogen side product, pulsing studies have shown drastic improvements in catalyst operating time, demonstrating stable eCO_2R performance of at least ten times longer.[31–34] The majority of eCO_2R studies reported to date have focused on constant-potential operation, and these potential-reversing studies establish anodic treatments and pulsed-potential methods as a promising approach to improve durability of the eCO_2R.[30,31,35–43]

More recently, similar pulse methods have garnered increasing attention as an attractive option to influence electrocatalytic processes and reaction selectivity beyond mainstream efforts to modify the catalyst and electrolyte.[32,44–57] These mainstream efforts include surface faceting, nanostructuring the catalyst, modifying the electrochemical cell design, including additives in the electrolyte to control the ionic environment and pH, as well as combining copper with other metals to create bimetallic catalysts.[5] Catalysts structured with predominantly (100) facets, high electrochemically active surface areas, and more undercoordinated sites can favor C_{2+} products.[5] Bimetallic catalysts can use the combination of chemical and electronic

eCO_2R one step closer to practical application. The insights shared here present scientific and technological opportunities beyond p-eCO_2R studies to other electrochemical technologies, in particular, ones involving competing reactions or electrode deactivation.

[1]Robert Frederick Smith School of Chemical and Biomolecular Engineering, Cornell University, Ithaca, NY 14853, USA

[2]Department of Materials Science and Engineering, Cornell University, Ithaca, NY 14853, USA

https://doi.org/10.1016/j.joule.2021.05.014

Please cite this article in press as: Casebolt et al., Pulse check: Potential opportunities in pulsed electrochemical CO_2 reduction, Joule (2021), https://doi.org/10.1016/j.joule.2021.05.014

properties of the two different metals advantageously to control adsorbates on the surface to favor specific products.[5] Changes in electrochemical cell design can increase CO_2 availability at the surface to increase reaction activity, and electrolyte modifications can be made to create high-pH environments that favor C_{2+} product formation.[5] All of these techniques have achieved significant advances in improving reaction selectivity and activity, though stability remains an issue, especially with nanostructured catalysts where some have been reported to experience degradation within tens of minutes.[58] A complementary approach to improving reaction performance is to pulse the applied potential, which, in addition to being a simple technique to apply without any complex syntheses or pre-treatments, can also enact changes in the reaction environment such as electrode restructuring, roughening, improved mass transport, and interfacial pH control to achieve goals similar to the work of catalyst and electrolyte modification. Another advantage of pulsing methods is that the applied pulse profile can be altered during electrolysis, creating a responsive system that can adjust to the needs of the user, which is not possible to do with the catalyst and electrolyte modification techniques. From a technoeconomic perspective, the viability of p-eCO_2R needs to consider the balance of the "cost" of lost production during the "off-" pulse relative to the benefit of (1) lower product separation costs (due to better selectivity) and (2) extended electrolyzer durability (due to reduction of electrode fouling). From a scientific perspective, despite the ostensible simplicity of using pulse profiles to tailor the electrochemical reaction, many foundational questions concerning the mechanism and underlying physicochemical processes remain. Recent pulse studies have shed light onto the underlying relationship between pulse profile and electrochemical performance.[32,44,46,48–50,52,53,56] These studies have elucidated some of the general principles underlying pulsed eCO_2R (p-eCO_2R); the emerging mechanistic picture involves a concerted interplay (arguably a symphony) between dynamic changes in surface adsorbates, mass transport, and changes in catalyst composition and structure (*vide infra*). In this review, we summarize the emerging understandings relevant to p-eCO_2R and the broad opportunity space for discovery and advances ahead. We have organized this "review and perspective" as follows: we first discuss general electrochemical considerations and then review past and present achievements with regards to p-eCO_2R, before diving into the specific aspects of physical processes and the reaction mechanism. We end by providing an outlook to both future scientific challenges and potential technological applications.

FUNDAMENTAL ASPECTS OF PULSED ELECTROCHEMICAL CO_2 REDUCTION (P-eCO_2R)

Figure 1 provides a schematic illustration of the basic physical and chemical aspects that need to be considered in heterogeneous electrocatalytic redox processes. We will first discuss the general principles and then the considerations related to the case of a transient (i.e., pulsed) applied potential. The physicochemical processes involved in heterogeneous electrocatalysis have different potential dependencies and span a range of time and length scales; which means that each of the processes detailed below has a different characteristic response to an applied potential. Since the reaction occurs at a heterogeneous solid-liquid interface in the case of aqueous eCO_2R, or at a three-phase gas-solid-liquid interface in the case of a gas diffusion electrode flow cell, mass transport of reactants and products between the bulk and the double layer must be considered, especially since eCO_2R is very sensitive to concentration polarization.[26] Within the double layer, species adsorption and relevant intermediate binding energies need to be considered.[26] The adsorbed species can then undergo reaction and may desorb. On the solid side of the interface, a

Please cite this article in press as: Casebolt et al., Pulse check: Potential opportunities in pulsed electrochemical CO_2 reduction, Joule (2021), https://doi.org/10.1016/j.joule.2021.05.014

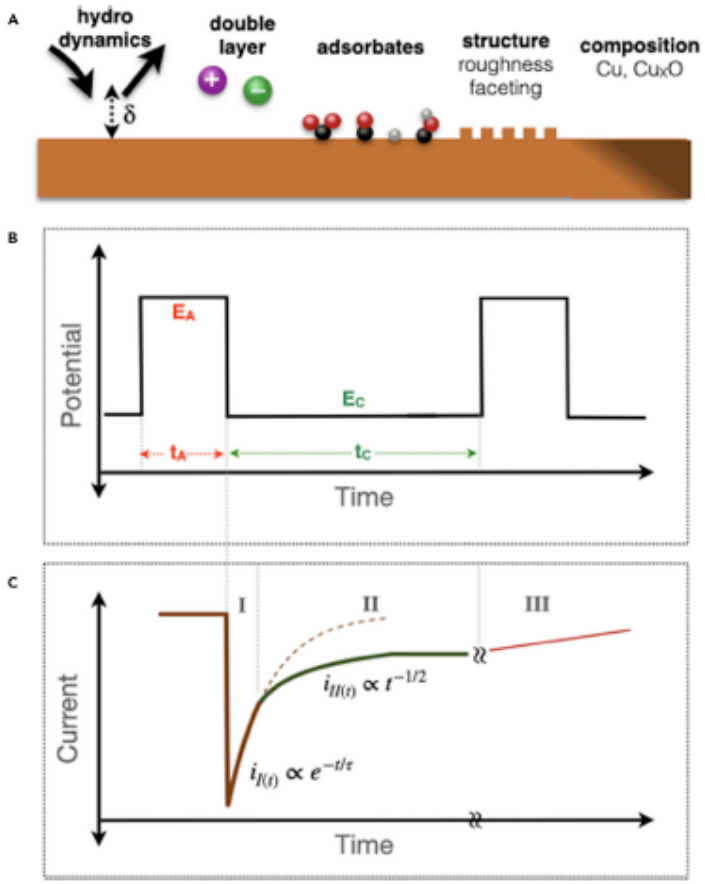

Figure 1. Physicochemical processes and dynamic current response in p-eCO$_2$R

(A) Overview of basic physicochemical processes involved in heterogeneous electrocatalysis that exist in dynamic equilibrium.

(B) Example applied pulse profile with important pulse parameters noted.

(C) Expected current response to an applied cathodic potential. (1) Capacitive charging current decays exponentially with time. (2) Faradic current decays with $t^{-1/2}$ in a diffusive system. (3) Catalyst deactivation/degradation resulting in a decrease in catalytic activity.

number of aspects need to be considered, including the electrode geometry and electrochemically active surface area (ECSA),[59,60] the detailed faceting and reconstruction,[5,19] and the catalyst chemistry (i.e., oxidation state and composition).[5,19,61] We note that although this review focuses on the specific case of pulsed electrochemical CO_2 reduction (p-eCO$_2$R), the effects of pulsing are generally applicable to other electrochemical processes, such as organic electrosynthesis,[62–70] or the processes of element extraction and contaminant removal[71–76] (see Section S1 for more information).

The recognition that each physicochemical subprocess illustrated in Figure 1A may occur at different intrinsic rates is essential to the p-eCO$_2$R thinking. As such, abrupt changes in applied potential have a significant consequence on the interplay

Please cite this article in press as: Casebolt et al., Pulse check: Potential opportunities in pulsed electrochemical CO_2 reduction, Joule (2021), https://doi.org/10.1016/j.joule.2021.05.014

between the subprocesses. The intention of pulsed potential methods is to manipulate these phenomena, for example, by applying an overpotential with frequencies comparable to the timescale of the subprocesses of interest. This strategy presents a simple and adjustable parameter (knob) to modulate the choreography of the dynamic interplay of mass transport, reaction kinetics, double layer charging/discharging, and surface adsorption/desorption.[77] In this way, we can create microenvironments that are inaccessible under potentiostatic conditions. Whereas a detailed description of the coupled transient processes during each pulse involves significant complexity, amid this complexity resides a compelling opportunity to tune and improve electrochemical processes.

The simplest form of a pulsed potential is the square wave profile shown in Figure 1B. We note that more complex waveforms (sine, asymmetric, sawtooth, etc.) are possible and likely offer additional tunability, once basic understanding of the relationship between pulse and electrochemical performance has been established. The pulsed electrolysis cell can be operated in galvanostatic (i.e., controlled current) or potentiostatic (i.e., controlled potential) mode. Figure 1B illustrates key control parameters in pulsed potential electrochemistry including the duration of the pulse, i.e., the anodic and cathodic pulse time (t_a and t_c) and the respective anodic and cathodic potential (E_a and E_c) applied during that time. The pulse duration, or time, can also be represented by the period of the cycle ($t_p = t_a + t_c$) or frequency ($1/t_p$). The pulse height is the magnitude of the pulse step, either in galvanostatic or potentiostatic mode. We note that the term "anodic" potential is used here to indicate the more positive potential of the two potential limits within the pulse sequence, although depending on its actual potential (relative to the potential of zero charge), the resulting current may be anodic or cathodic in nature. The value of the anodic potential is especially important in determining whether the catalyst experiences oxidation or just double layer rearrangement during the anodic pulse (discussed more below).

The transient cathodic current response of the aqueous electrolytic cell in response to a cathodic step change in the applied potential is schematically illustrated in Figure 1C. We can categorize the dynamic transient current profile into three temporal regimes (I–III).

(1) The immediate response to a change in applied potential is the reorganization of the electrical double layer (EDL). In a non-adsorbing condition, one can use the Guoy-Chapman-Stern model to understand how the EDL changes in response to the application of the potential pulsing.[78] In the limit of highly concentrated electrolyte, the ions behave like an ideal capacitor, which contributes non-faradic charging current. This capacitive charging current decays exponentially with a characteristic time, similar to the charging current encountered when a potential step is applied to a series RC circuit (Figure 2).[79] The situation is more complex when specific adsorption is possible. Notably, the resulting EDL becomes a balance between the chemical and electrical potential of the interfacial species. It is not straightforward to describe the general EDL behavior under this condition, as the adsorption depends on the electrode chemistry as well as on the applied potential. Furthermore, the movement and adsorption rates are chemistry dependent, further increasing the complexity of the EDL.

The identity of ions presents in the EDL, which is potential dependent, affects eCO_2R activity and selectivity through cation promoter effects, buffering, and specific

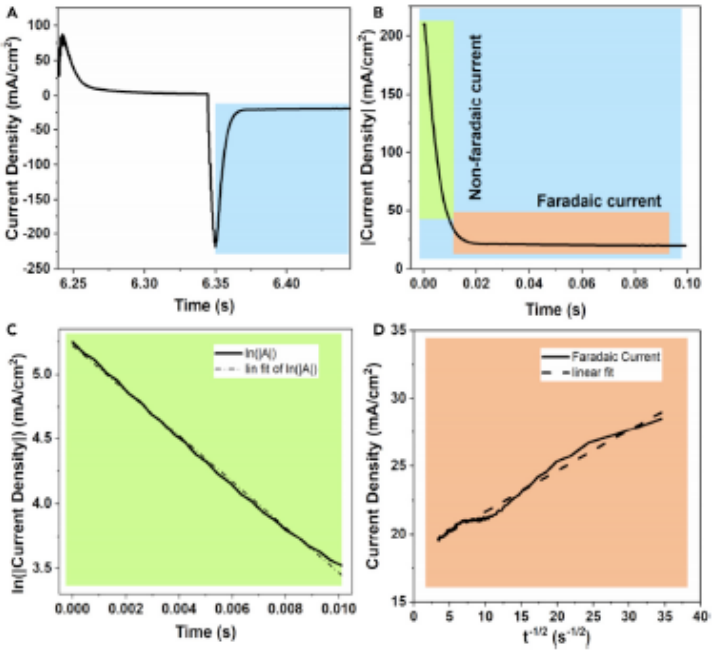

Figure 2. Separating current contributions into non-faradic and faradic current following the application of a potential pulse

(A) Full pulse profile of a 100 ms pulse ($t_a = t_c$).

(B) Absolute value of cathodic current from the blue inset.

(C) Natural log of the absolute value of the non-faradic current from the green inset with a linear fit.

(D) Faradic current from the orange inset with a linear fit. Reproduced from Kimura et al.,[44] with permission.

adsorption, which we will briefly mention here. Large cations such at Cs^+ have the smallest hydrated cation radius and therefore have the smallest repulsion close to the electrode.[80] This allows for a higher cation concentration at the surface, leading to a large surface charge density and stronger interfacial electric field, which increases CO_2 adsorption and enhances C_2 production.[80–82] Electrolyte anion identity and buffering capacity have also been suggested to buffer the interfacial pH, which determines the reaction selectivity and activity.[83] Resasco et al. found that buffering anions favor protonated products by instead serving as hydrogen donors.[84] Specific adsorption of anions in the double layer has also been shown to impact product selectivity, with observations of hydrogen suppression as a result of Cl^- adsorption.[85] Studies exploring the effects of different anions have found that anion co adsorption can modify the *CO binding energy and the electronic structure of local catalyst sites to promote C–C coupling.[86] Double layer rearrangement effects after the application of a potential typically happen on the order of milliseconds.

While we will not discuss all of the mechanistic complexities of EDL here, we point out the opportunity to use pulsing to fine-tune this complexity to build the best microenvironment possible for eCO_2R.

(2) The transition from the initial non-faradic charging to the subsequent faradic current can be analyzed with quantitative rigor as illustrated in Figure 2. Following the

Please cite this article in press as: Casebolt et al., Pulse check: Potential opportunities in pulsed electrochemical CO_2 reduction, Joule (2021), https://doi.org/10.1016/j.joule.2021.05.014

initial exponential decay in current (within a characteristic time defined by the RC time constant), the subsequent transient regime is characterized by an I-versus-$t^{-1/2}$ response (Figure 2D). This regime reflects the faradic current due to the flow of electrons across the electrode/electrolyte interface (redox reaction) in a diffusive system, i.e., where kinetics is not the limitation. This transient can be described by the Cottrell equation.[45] At shorter times, the current described by the Cottrell equation decays rapidly, and at longer times, the current tends toward a limiting value. In eCO_2R, efforts to increase the limiting current involve increasing CO_2 solubility in solution (by modifying operational temperature and pressure or by using different electrolytes like ionic liquids) or by using pure CO_2 feed gas in a gas diffusion electrode configuration.

(3) If the potential is applied for an extended period (several seconds to hours), a third regime may be entered in which the electrochemical current decreases due to degradation or deactivation of the catalyst surface. Catalyst deactivation can be generally separated into three causes: chemical, mechanical, or thermal degradation.[87] In eCO_2R, important degradation pathways with respect to Cu-based catalysts include fragmentation, Ostwald ripening, dissolution, detachment, agglomeration, reshaping, or poisoning.[58] Poisoning species include impurities from the electrolyte, glassware, CO_2 feed stream, reference or counter electrodes, and others, or eCO_2R intermediates irreversibly bound to the surface.[28,29,88–91] These processes cause changes in the structure, morphology, and ECSA, which in turn change the catalytic activity as well as modify the reaction selectivity.

It is important to note that upon the application of an anodic potential, there is a similar current response as reported in Figure 1B, following the application of a reducing potential including non-faradic current due to double layer reorganization, faradic current due to CO_2 reduction or due to copper oxidation depending on the applied potential, and the possibility of catalyst poisoning depending again on the applied potential.

Consideration of these three temporal regimes thus points toward a timing "window of opportunity." In the language of the domains illustrated in Figure 1C, this timing window of opportunity refers to regime II. To make an informed decision about optimal pulse duration, one should therefore select a pulse that is (1) sufficiently long such that the majority of the current goes to faradic processes instead of double layer charging, but (2) not too long such that the current drops due to poisoning of the catalyst active sites.

To ensure that the pulse duration is sufficiently long to neglect the influence of double-layer charging, one needs to approximate the characteristic double-layer charging time. The relative importance of the non-faradic charging current compared with the faradic processes depends on the relative duration of the pulse compared with the capacitive charging time. For shorter pulse times, with a predominant portion of the pulse spent in regime I, the majority of current is used for double-layer charging, which reduces the process efficiency with which current is used to reduce CO_2. The RC time constant (i.e., the time required for charge equilibration of the double layer) depends on the cell resistance and the capacitance of the electrode, both of which depend on the electrode area, applied potential, ionic concentration, and other experimental parameters.

By selecting a cathodic pulse duration in regime II and avoiding regime III, one can regenerate the catalyst before loss of activity due to poisoning to ensure longevity of

Please cite this article in press as: Casebolt et al., Pulse check: Potential opportunities in pulsed electrochemical CO_2 reduction, Joule (2021), https://doi.org/10.1016/j.joule.2021.05.014

the system. Moreover, "fine tuning" the cathodic pulse duration and applied pulse potential within regime II provides a compelling opportunity to modulate dynamic interplay of transport, adsorption, and reaction. The choice of applied potential and duration is equally important during the anodic pulse, since the choice for E_a can result in changes in the adsorbates in the double layer, copper oxidation, and electrode reconstruction, all of which can have persistent effects throughout the entire pulse cycle. "fine tuning" the cathodic and anodic pulse durations and potentials provides additional control over product selectivity during electrolysis (beyond what is possible by pre-engineering the catalyst and electrolyte). In context of the resurging interests in electrochemical methods, particularly CO_2 reduction, we note that there are many more opportunities ahead. We anticipate that emerging insights into pulse design principles (i.e., the underlying relationship between product selectivity and pulse profile—pulse shape, duration, and potential) will spur on future advances in pulsed electrosynthesis.

Summary of pulsed electrochemical CO_2 reduction (p-eCO_2R) experiments

Whereas the first reports of eCO_2R date back to 1954,[92] the application of anodic treatments was not investigated until 1990.[35] Early pulsed potential methods have focused on relatively long interval (i.e., seconds to minutes) pulses aimed predominantly at avoiding catalyst degradation by restoring the activity of the electrode surface through the anodic potential application. The application of shorter (i.e., millisecond) pulses to tailor the product selectivity only emerged recently.[48] Below, we will first provide a synopsis of the recent p-eCO_2R studies (tabulated at the end of this section). We organize the summary by pulse duration to reveal the role of the mechanisms at different timescales. Then, we go on to discuss the emerging understanding of the underlying mechanism in the following section.

"Long" pulses (>1s)

In 1990, Wasmus et al. demonstrated that periodic anodic pulses could be used to recover Cu electrode appearance and activity.[35] They interpreted the periodic anodic pulse as a means to reverse graphitic deposition, which was known to deactivate the electrode surface under constant-potential electrolysis.[28] Subsequent reports by Shiratsuchi, Nogami and co-workers systematically studied p-eCO_2R on Cu and Ag electrodes.[30,36,38] Their studies demonstrated that 5-s pulses applied to Cu electrodes prevented graphite deposition and sustained hydrocarbon formation. They reasoned that periodic anodic pulses oxidize adsorbed intermediates (formic acid and/or formate) and thereby avoid the formation of inactive graphitic deposits.[30] Moreover, their *ex situ* X-ray photoelectron spectroscopy (XPS) measurements revealed that anodic pulses led to the formation of a thin Cu_2O film. A subsequent study by Jermann and Augustynski applied CV scans in 5-min intervals and also observed stable eCO_2R.[31] Beyond confirming the role of the periodic anodic potential in hindering the adsorption of inactive amorphous carbon, Jermann and Augustynski also observed a shift in product selectivity. Like previous reports, they too suspected the role of oxidized species, suggesting that these persistent Cu^+ regions favor ethylene.

A 1996 p-eCO_2R study on Ag electrodes by Shiratsuchi et al. suggested that the pulsed potential influences the CO_2 adsorption, as well as proton affinity, thereby impacting product selectivity.[38] In 2000, Ishimaru et al. studied p-eCO_2R on Cu/Ag-alloyed electrodes and argued that by controlling the pulse profile and the alloy ratio, they could control the amount of adsorbed CO on the surface and thereby tailor product selectivity.[37] In a similar effort to use pulsing to control the adsorbed CO population on the surface, Lee and Cho et al. found that pulsing on Pd-based

Please cite this article in press as: Casebolt et al., Pulse check: Potential opportunities in pulsed electrochemical CO_2 reduction, Joule (2021), https://doi.org/10.1016/j.joule.2021.05.014

catalysts could stably produce formate over the course of 45 h.[33] Poisoning by strongly adsorbed CO species can cause Pd catalysts to degrade. However, pulsed electrolysis selectively oxidizes CO, removing it from the surface and thereby enhancing eCO_2R to make formate.

To understand the effects of p-eCO_2R, in 1997, Friebe et al. examined pulsing on copper using differential electrochemical mass spectrometry (DEMS) to confirm stable eCO_2R activity over time, suggesting that pulsing reverses the poisoning pathway.[40] In 2001, Lee and Tak used electrochemical quartz crystal microbalance (EQCM), which simultaneously measures mass change and current flow, to study p-eCO_2R on copper.[41] During constant eCO_2R, they observed an increase in the mass of the electrode, while the production of methane simultaneously decreased. They were able to identify this mass increase as deposited graphite (using *ex situ* scanning electron microscopy [SEM] and AES), which deactivated the electrode over time. This study revealed that pulsed potentials successfully mitigated any precipitation of graphite. Using *ex situ* XRD, they observed Cu_2O on the surface, postulating that Cu dissolves during the anodic pulse, which then reacts with local hydroxides to precipitate Cu_2O on the surface and thereby preventing carbon poisoning.[41]

A 2007 study by Yano et al. evaluated potential pulsing on Cu and Cu_2O electrodes and demonstrated that optimization of the anodic pulse potential and duration enhances the selectivity (i.e., faradic efficiency, the efficiency with which electrons are transferred) of ethylene.[93] They interpreted the fact that the enhancement in ethylene selectivity observed with pulsing was more pronounced on Cu_2O than on Cu electrodes as an indication that the Cu_2O phase prevents immediate protonation of adsorbed CO intermediates, thereby allowing for C–C coupling and increased ethylene selectivity. In 2016, Lim et al. studied the effect of periodic CV scans and potential steps on the performance of galvanostatic eCO_2R on Cu.[51] By applying this anodic treatment every 2 h, they showed that they could favor the production of CO at the expense of methane. From this result, the authors suggested that they were switching between the two surface coverages determined by the competitive intermediate adsorption.

New insights into the role of pulsed potentials and long-term stability were reported in a 2018 study by Engelbrecht et al.[32] Their pulsed electrolysis study demonstrated 95 h of stable p-eCO_2R performance, reiterating that pulsing mitigates catalyst poisoning. To understand the role of pulsing in creating durable electrode activity, they monitored changes in the catalyst surface structure using SEM and found that applying a more negative upper potential conserved the surface structure, whereas more positive upper potentials led to increasing surface rearrangement. Under pulse profiles in which the upper potential was above the open-circuit potential, the electrode structure was observed to corrode, with material being deposited onto the electrode surface and in the catholyte. Based on these insights, they advised that the anodic pulse potential be chosen to create favorable surface modifications, while avoiding material dissolution.

The relationship between pulse profile, electrode structure, and product selectivity was recently illustrated by Jiang et al. who used pulsing to synthesize an electrode for eCO_2R.[94] They cycled a Cu foil electrode 100 times between an upper and lower potential and found that cycling resulted in arranged nanocubes that exhibited high ethylene selectivity when tested under potentiostatic conditions. They attributed this observation to electrode roughening, which increases the reaction rate per geometric surface area. This led to an increase in local pH, which consequently

Please cite this article in press as: Casebolt et al., Pulse check: Potential opportunities in pulsed electrochemical CO_2 reduction, Joule (2021), https://doi.org/10.1016/j.joule.2021.05.014

suppressed the competing hydrogen evolution reaction (HER) in favor of C_2 product formation. Even though we are focusing on pulsed potential electrolysis and in this case, they used pulsing only for electrode synthesis, their findings offer additional insight into the effects of pulsing and what structural changes can be taking place during p-eCO_2R.

Advances in *in situ* and *operando* spectroscopy characterization methods have been very beneficial to efforts focused on decoupling the complex transient processes in p-eCO_2R. A study by Lin et al. used *operando* seconds-resolved x-ray absorption spectroscopy (XAS) to track the chemical state evolution of their mixed-valence oxide-derived copper catalysts.[53] Whereas observing no changes in morphology with TEM measurements under pulsed potential conditions (-1.15 V < E_c < -0.7 V versus RHE, E_a = 0.5 V, t_a = t_c = 10 s), they found that their catalysts achieved a steady state between half Cu^0 and half Cu^+ species, which selectively produced ethanol. Supplementing their experimental observations with DFT calculations, Lin also suggested that the co-existence of Cu^+ and Cu^0 under pulsed conditions enhanced OH species present at the boundary, which stabilized carbonyl intermediates, thereby preventing protonation of the terminal oxygen site and allowing oxygenated CO_2R product formation.

A 2020 study by Kim et al. tracked the temporal evolution of p-eCO_2R products over time on Cu using DEMS.[56] The researchers hypothesized that CO accumulates on the Cu surface during the cathodic sweep, and that this inventory of adsorbed CO subsequently reduces to C_2H_4 or desorbs as CO during the anodic sweep. Owing to DEMS with a time resolution of less than 0.5 s, Kim et al. were able to differentiate between transient and steady-state behaviors. By pulsing far below the Cu oxidation potential (E_c = -1.15 V versus RHE; E_a = -0.8 V; t_c = 5, 10, and 25 s; t_a = 5, 10, and 60 s), they ruled out oxidation, and based on insights from the SEM images, they ruled out morphological changes. Another interesting discovery enabled by the fast time resolution of DEMS was that over time during p-eCO_2R, the local concentration of ethylene increased, and the concentrations of CO and H_2 decreased as pulsed operation went on. They attributed improved C_2 selectivity under pulsed conditions to the enhanced surface concentration of CO versus H, which improved C–C coupling and suppressed HER.

In a time-dependent continuum model, Bui et al. tracked the effects of pH and CO_2 concentration in the boundary layer on the kinetics for forming individual products to understand why C_{2+} product formation is enhanced under pulsed conditions.[95] Modeling a variety of different pulse profiles in 0.1 M $CsHCO_3$ ranging from 5–20 s pulses, they were able to reproduce experimentally observed results by Kim et al.,[56] and proposed that a transient state of heightened pH, CO_2 concentration, and driving potential under pulsed conditions are responsible for improved eCO_2R performance. Testing a range of pulse shapes (modifying pulse amplitude, width, and duty cycle), they showed that more cathodic pulse amplitudes lead to higher current densities, but that too high of an overpotential favors methane formation over C_{2+} products. They also showed that shorter pulse widths improve current density and enhance C_{2+} FE, since the fraction of time spent in the state of increased pH, CO_2 concentration, and overpotential is increased; however, too short of a pulse time is limited by double layer charging. This work further highlights the importance of understanding and controlling the reaction microenvironment under pulsed conditions.

Considering the myriad of dynamic processes on the electrolyte side of the electrode-electrolyte interface, the composition and concentration of the electrolyte

Please cite this article in press as: Casebolt et al., Pulse check: Potential opportunities in pulsed electrochemical CO_2 reduction, Joule (2021), https://doi.org/10.1016/j.joule.2021.05.014

should also impact the p-eCO_2R response. Oguma and Azumi examined the effects of pulsing on silver (Ag) in an electrolyte solution containing ionic liquids (1-ethyl-3-methylimidazolium ethyl sulfate (EMISE)).[55] Under pulsed conditions (E_c = −1.4, −1.5, and −1.6 V versus Ag/AgCl for 5 s, and E_a = 0 V for 5 s), they observed that the formation of CO relative to H_2 was considerably higher than that obtained during potentiostatic electrolysis. Adding EMISE to their bicarbonate electrolyte further improved CO selectivity. The main conclusion of their work was that pulsing mitigated the evolution of a CO_2 reactant depletion layer (whether or not EMISE was present), while EMISE further enhanced reactant concentration at the interface by complexing CO_2 more strongly to the surface. Recent work from our group (Casebolt and Kimura et al.) showed that the relationship between electrolyte concentration/composition and product distribution for short (i.e., 50 ms) pulsed potential eCO_2R is different from constant-potential eCO_2R, due to the differences in reaction environment between pulsed and static eCO_2R.[45] Under static conditions, increasing the electrolyte buffer concentration has been shown to significantly increase hydrogen formation and slightly increase methane formation, while under pulsed conditions, we find that HER is suppressed at all bicarbonate concentrations (0.1–1 M $KHCO_3$) as a result of the preferential hydrogen desorption during the anodic pulse, whereas methane selectivity is significantly enhanced at increasing bicarbonate concentrations.[45] Recent modeling work by Bui et al. also showed a significant increase in methane selectivity when pulsing at increasing $CsHCO_3$ concentrations, reiterating our experimental observations.[95] Using our experimental parameters in the 1D continuum model developed by Gupta et al.,[43] we rule out differences in pH and instead suggest that bicarbonates role as a proton donor is the reason for increased methane selectivity at increased buffer concentrations.[45,84] We also explored the effects of increasing concentration in the unbuffered KCl electrolyte under static and pulsed conditions and found that under static conditions, there is no change in selectivity with both hydrogen and CO being the main products. However, at increasing KCl concentrations under pulsed conditions, C_2 selectivity is significantly increased, reaching over 70% FE. We hypothesize that C_2 products are favored at higher KCl concentrations because of the higher flux of CO_2 to the surface (using Cottrell analysis), which increases CO_{ads} coverage, and the higher concentration of OH at the surface stabilizes the CO_{atop} intermediates to promote C–C coupling.[45,46] This work highlights how pulsing can be used to control the microenvironment (through preferential H_{ads} desorption and OH adsorption), as well as how the proton donor ability of the electrolyte determines the product selectivity. This is just the beginning of understanding electrolyte effects in p-eCO_2R, and there is a lot more room for exploration.

p-eCO_2R has proved advantageous beyond application in liquid cells. Lee et al. recently examined the effect of periodic anodic treatments on gas diffusion electrodes (GDEs) operated at high current densities (> 80 mA/cm^2).[54] Using a custom-built, gas-fed *operando* XAS cell coupled with gas chromatography (GC) measurements, Lee explored the relationship between the Cu-based catalyst oxidation state and the ethylene activity during CO reduction. Using two different periodic anodic treatments ([1] apply 1.5 or 0.1 V versus Ag/AgCl for 5 min after bulk electrolysis at −2.2 V for 1 h, or [2] scan 20 times between −1.1 and 0.5 V at 50 mV/s), they found no correlation between Cu oxidation state and ECSA to ethylene production. Using *ex situ* microscopic techniques, they suggested that ethylene activity improves with oxidative treatment because of morphological changes (their nanostructures coalesced into smooth surfaces during electrolysis independent of initial oxidation state or starting morphology, and then the nanostructures were regenerated after anodic treatment) that generate more active structures. Consistent with

Please cite this article in press as: Casebolt et al., Pulse check: Potential opportunities in pulsed electrochemical CO_2 reduction, Joule (2021), https://doi.org/10.1016/j.joule.2021.05.014

previous studies, they found that anodic treatments improved catalyst stability, noting that their results show a technique for cell regeneration that can restore catalyst performance without cell disassembly, thereby mitigating gas-fed GDE cell degradation.

Another recent study testing the efficacy of pulsing in a flow cell configuration, by Jännsch et al., found that pulsing enables stable ethylene production over the course of 16 h and that pulsing can recover the activity of deactivated electrodes.[57] While no characterization techniques were employed, they suggested that pulsing stabilizes active catalyst facets, probably through active surface reconstruction as proposed by Arán-Ais et al.[52] Another recent study by Xu et al. showed that pulsing can be used in a membrane electrode assembly as a self-cleaning strategy to avoid carbonate salt formation.[34] High current density electrolysis produces large quantities of hydroxide ions on the cathode, which react with potassium and carbonate ions (present in excess because of the high pH) to form salt precipitates that hinder CO_2 mass transport and destabilize cell performance. By carefully choosing a regeneration voltage, Xu et al. were able to momentarily halt hydroxide formation while maintaining an electric field which facilitated carbonate migration to the anode. This enabled the cathode to never reach the potassium carbonate solubility limit, which prevented salt formation and resulted in 236 h of stable operation at 138 mA/cm^2 with 80% C_2 product selectivity. In a study published earlier this year study, Jeon et al. demonstrated that pulsing modifies selectivity on copper nanocubes in a gas-fed flow device, observing a 10% enhancement toward C_2 products (reaching C_2 FE ~64% at E_a = 0.9 V versus RHE) under pulsed conditions compared with potentiostatic conditions at current densities > 250 mA/cm^2.[96] They attributed the enhanced selectivity toward ethylene and ethanol to irreversible morphological reconstruction resulting in a highly defective interface with more grain boundaries. Interestingly, as they pulsed to more anodic potentials, they observed decreasing selectivity toward C_2 products, which they attributed to OH^- consumption at the surface (forming a Cu_2O shell), resulting in an OH-poor environment that favors methane production. These studies indicate that pulsing has advantageous effects in not only aqueous cells, but in high current flow cell configurations required for industrial-scale implementation.[34,54,57,96]

"Short" pulses (<1 s)

We now turn our attention to shorter, sub-second pulses. To our best knowledge, the first study of sub-second pulses was reported in 2016 by Kumar et al. who demonstrated that the application of millisecond (square wave) pulses had a significant impact on the CO_2R product selectivity on Cu, observing only H_2 and CO.[48] They speculated that the rapidly changing local electric field near the interface significantly affects the binding energy experienced by adsorbed intermediates leading to desorption of CO before it can reduce further to hydrocarbon products, as well as inhibiting the binding of CO_2 which results in HER promotion over CO at very short pulse times (<50 ms). They also suggested that *in situ* oxidation and reduction of Cu preferentially formed CO over other carbon products, resulting in tunable syngas formation.

A subsequent study employing millisecond pulses on copper electrodes by Kimura et al. reported the selective formation of methane for all pulse intervals, as well as significant HER suppression.[44] Although both studies by Kumar[48] and Kimura[44] used similar pulse times, potentials, and electrolyte, the variations in reported product selectivity reveal remarkably different responses of the product selectivity to pulsed potential. Whereas Kumar reported enhanced HER under millisecond pulse

https://doi.org/10.1016/j.joule.2021.05.014

conditions, Kimura reported the opposite trend finding that millisecond pulses suppressed HER. This difference underscores the critical role of the relative magnitude of the non-faradic and faradic transient currents during regimes I and II (see Figure 1). The differences in induction time and double layer charging rate are directly related to differences in electrode area. Whereas Kimura used 0.1 cm^2 electrodes (observing H_2 suppression and CH_4 enhancement), Kumar used 5 cm^2 electrodes (observing only H_2 and CO production). With larger electrodes and slower RC response times, a relatively large fraction of the millisecond pulse is spent charging the double layer, i.e., the potential profiles at the electrode-electrolyte interface were not identical. This comparison highlights that to enhance eCO_2R product formation under pulsed conditions, it is crucial that the electrochemical system has a sufficiently fast response time to cycling potential.[44] Breaking this down further, configuring the electrolysis cell to ensure relatively fast RC response time by reducing the ratio of electrode size to pulse time, minimizing cell resistance, and taking into account the optimal positioning of the reference electrode is essential to creating a reproducible application of pulsed potential. Further, we propose that in high current devices with high ohmic drops and high catalyst surface areas, the pulse duration will need to be scaled accordingly so that the ratio of pulse duration to charging time remains relatively "fast."

Further insights into the relationship between pulsed potential and product selectivity emerged from a 2017 study using online electrochemical mass spectrometry by Le Duff et al.[47] Using pulsed voltammetry (stepping between −0.2 and −1.1 V versus RHE at 10 Hz) to track CO_2 reduction products over single crystal, Cu(111) and Cu(100) electrodes, Le Duff showed that oxygenated hydrocarbons were formed more favorably under alternating conditions. The authors attributed this higher product selectivity toward oxygenated hydrocarbons to the enhanced surface coverage of oxygen species (OH_{ads}) during the pulse.

To understand the role of defect structures and oxidation state during p-eCO_2R, Arán-Ais et al. tracked the surface composition of single crystal copper electrodes as a function of the anodic pulse potential (varied between 0 and 0.8 V versus RHE) and cathodic pulse duration (varied between 0.2 and 1s) using *quasi in situ* XPS.[52] This careful work allows a correlation between surface characteristics and product selectivity They found that ethanol is favored when more Cu^+ is generated during the anodic pulse, and that ethylene has no dependence on Cu^+ concentration. Instead they found that ethylene depends on the length of Cu(100) domains. They also observed no significant changes in ECSA during the pulse program.

In a follow-up study by Tang et al., using (100)-textured polycrystalline copper foil, they too found that pulsing enhanced C_{2+} product formation.[97] While Arán-Ais et al. found that Cu^+ stabilization during pulsing enhanced ethanol formation without affecting ethylene production,[52] Tang et al. demonstrated that the factor controlling selectivity between ethanol and ethylene is the reduction rate of the Cu^+ during the cathodic pulse, which they modified through temperature control. By decreasing the temperature to 5°C, thereby slowing the reduction kinetics, Tang et al. were able to achieve 40% selectivity to ethanol because the active Cu^+ species from the anodic pulse persisted through the cathodic pulse. Furthermore, they showed that the competition between ethylene and ethanol corresponds proportionally to the response time of the reduction cycle, providing insight into how temperature control can be used to tailor C_2 selectivity.

Please cite this article in press as: Casebolt et al., Pulse check: Potential opportunities in pulsed electrochemical CO_2 reduction, Joule (2021), https://doi.org/10.1016/j.joule.2021.05.014

Both Strain et al. and Kimura et al. demonstrated that in addition to improving eCO_2R performance, pulsing also improves CO reduction compared with HER.[44,46,49] The fact that the pulsing mechanism enhances performance even when starting from CO demonstrates that the influence of pulsing is not specific to the first eCO_2R intermediates ($*CO_2^-$, *COOH).[5,98,99] Strain et al. examined pulsed CO reduction on oxide-derived Cu electrodes under a range of pulse conditions ($E_c = -0.35$ V, $E_a = 0$ V versus RHE, 0.01 s $\leq t_a = t_c \leq$ 50 s) and showed that product selectivity depended on pulse duration.[49] Application of short ($t \leq 1$ s) pulses resulted in the reduction being selective to the COR, specifically increasing selectivity toward C_1 products over C_2 products, and suppressing the HER. They suggested that non-faradic charging dominates at short pulse times and that the continually changing surface energetics prevent adjacently adsorbed CO species from binding.

To better understand the physicochemical processes within the double layer during pulsing, a 2020 paper by our group (Kimura et al.) examined p-eCO_2R on polycrystalline copper using *in situ* XPS supplemented by a multi-species Langmuir isotherm model.[46] Using millisecond pulses and testing a range of pulse potentials, Kimura et al. found that pulsing selectively improved CO_2R products over HER compared with the constant-potential eCO_2R when $E_a \geq 0.2$ V versus RHE ($E_c = -1.05$ V, $t_a = t_c = 50$ ms). When $E_a \geq 0.2$ V, we also found that the baseline anodic current (i_a) > 0 mA/cm^2, indicating the existence of an oxidative reaction. While copper oxidation could be behind this oxidative reaction, another possibility is that pulsing changes the composition of adsorbates at the interface, notably, the electro-adsorption of hydroxides ($H_2O \rightarrow OH_{ads} + H^+ + e^-$). These adsorbed hydroxides could promote the CO_{atop} formation while preventing the CO_{bridge} formation that could deactivate the Cu surface. We proposed that this CO_{atop} formation leads to the favorable competition between CO_{ads} and H_{ads} to suppress the HER. *In situ* X-ray absorption near edge structure (XANES) revealed that $Cu(OH)_2$ was formed at a constant potential of 0.2 V versus RHE. However, the application of short (50 ms) pulses to $E_a > 0.2$ V did not lead to any detectable $Cu(OH)_2$. These spectroscopic insights show that pulsing enables the electrode to undergo an oxidation reaction without causing bulk copper oxidation, provided that the cathodic potential is sufficiently reductive (< −0.8 V). In this window with no bulk oxidation, improved CO_2R is due to the changes within the interface (i.e., the active adsorption/desorption of ions). A three-part experiment going from pulsed reduction, to constant reduction, back to pulsed reduction with corresponding switches in observed selectivity further supported that pulsing is a reversible and transient treatment that cannot be explained by permanent surface reordering. And the four component (OH_{ads}, H_{ads}, CO_{bridge}, CO_{atop}) Langmuir model showed that pulsing favors OH_{ads} accumulation consistent with the findings of Iljima et al.[100] Over long times (100–1,000 s), pulsing maintains CO_{atop} coverage compared with constant reduction where CO_{atop} slowly transforms to inactive CO_{bridge}. The cathodic potential maintains the reduced state of copper and creates a high pH surface environment where residual OH^- remains on the surface, inducing near neighbor coupling interactions with CO_{ads}, thereby favoring CO_2R products and suppressing HER.

A 2020 report by Blom et al. evaluated p-eCO_2R methods on lead (Pb) electrodes, further demonstrating the utility of the p-eCO_2R beyond that of copper.[50] Whereas lead electrodes typically deactivate after 30 min under potentiostatic conditions, pulsing enabled stable formate production for 16 h. Blom et al. examined symmetric and asymmetric square wave pulses and found that high frequency pulse cycles (cycle time = 0.002 s) were dominated by double layer charging and that this fast reoxidation of intermediates inhibited formate production. Using longer cycle times

Please cite this article in press as: Casebolt et al., Pulse check: Potential opportunities in pulsed electrochemical CO_2 reduction, Joule (2021), https://doi.org/10.1016/j.joule.2021.05.014

(cycle time = 0.02 to 0.2 s), they observed significant increases in formate partial current density and selectivity. *In situ* Raman spectroscopy revealed that the Pb surface oxidizes to form $PbCO_3$ during the anodic pulse which is hypothesized to be more active toward formate production, and that the Pb^{2+} reduces back to Pb^0 during the cathodic pulse.

Pulsing in eCO_2R has been used to prolong electrode lifetime and modulate product selectivity. Comparing trends between these various studies is not trivial as each group uses different electrochemical procedures, equipment, experimental conditions, and analysis methods. In an effort to make comparisons easier, we have included a table below outlining the conditions under which each experiment was run, including major observations and hypotheses (Tables 1 and 2). Despite differences in experimental parameters, several major mechanisms have been proposed, including surface oxidation, catalyst reconstruction, improved reactant concentration in the double layer, and changes in surface adsorbate coverage.

MECHANISTIC INSIGHTS INTO (P-eCO_2R)

Building on the summary of experimental results discussed above, we now turn our attention to describing the underlying mechanisms and the interplay between competing dynamic subprocesses previously illustrated in Figure 1A. We recapitulate our main hypothesis that differences in characteristic timescales and potential dependencies of competing subprocesses can be exploited through the judicious design of the pulse profile. The result is the ability to influence the reaction pathways and thereby tune product selectivity and catalyst longevity. Our intent here is to illustrate initial insights into the complex interplay between these processes and to inform the relative magnitude of their contribution rather than to identify the singular determinant. Pulsing improves catalyst lifetime and performance stability.[5,101] Whether it be impurities from some part of the electrolysis cell or irreversibly adsorbed intermediates and CO_2R products (graphite), pulsing reverses these deactivation pathways thereby prolonging catalyst lifetime. However, despite these observed benefits, the mechanism by which pulsing modifies the eCO_2R is still an open question. We have organized the mechanistic discussion below along the lines of the key processes illustrated in Figure 1A. In separate studies, processes within the boundary layer (i.e., hydrodynamics and mass transport),[43,55,56] at the electrode surface (i.e., adsorbates),[37,38,44,46–49,51,53,56] and within the electrode (i.e., structure and composition)[30–32,36,37,39,41,42,48,50,52–54,57,94] have been evoked to explain observed trends. It is important to recognize that these processes do not operate in isolation but rather in concert at the pulsed solid/electrolyte interface, so while we cannot rule out any process completely, we can speak about its relative contribution in different pulse conditions.

Hydrodynamics and the role of mass transport limitations

As with any liquid-phase electrochemical reaction, mass transport of the reactants from the bulk fluid to the electrode interface requires careful consideration. Fast surface reaction rates will deplete the reactant near the surface and result in concentration polarization (i.e., spatial gradients of the reactant concentration from the catalyst surface to the bulk fluid). In this mass transport limited regime, the overall reaction rate is limited by the transport (diffusion, migration, and convection) of reactants through the boundary layer to the active site (regime II, Figure 1C). Mass transport limitations are more pronounced for reactions at higher current densities where reactants are more rapidly consumed, though this can be overcome by optimizing electrolysis cell design or using gas-fed devices. In eCO_2R, the overpotentials

Please cite this article in press as: Casebolt et al., Pulse check: Potential opportunities in pulsed electrochemical CO_2 reduction, Joule (2021), https://doi.org/10.1016/j.joule.2021.05.014

Table 1. "Long" pulses (>1 s)

Catalyst	Electrolyte[a]	Anodic treatment				Stability	Selectivity[b]	Effect of anodic treatment	Hypothesis	Ref.
		E_c, I_c	t_c	E_a, I_a	t_a					
Cu (12.3 cm^2)	0.5 M $KHCO_3$	stepped to −1.50 mV versus SCE from E_c for no longer than 1 min, $-0.6\ V \geq E_c \geq -2.4\ V$ versus SCE				-	-	partially recovered electrode's metallic appearance and almost all of its catalytic activity	inhibition of poisoning	Wasmus et al.[35]
Cu (1 cm^2)	0.1 M $KHCO_3$	−1.8 V versus SCE	1–9 s	0 V versus SCE	1–9 s	25 h	H_2 ~ 20%, CH_4 ~ 10%, C_2H_4 ~ 25%	constant CH_4 and C_2H_4 selectivity and HER suppression, as well as long-term stability	inhibition of poisoning and surface oxidation	Shiratsuchi et al.[30]
Cu (1 cm^2)	0.1 M $KHCO_3$	$-1.6\ V \geq E_c \geq -3.4$ V versus SCE	5 s	$0.2\ V \leq E_a \leq 1.5$ V versus SCE	5 s	4 h	H_2 ~ 30%, CH_4 ~ 30%, C_2H_4 ~ 15%	selectively produce hydrocarbons based on choice of E_a and long-term stability	surface oxidation	Nogami et al.[36]
Au (0.2 cm^2)	0.1 M $NaHCO_3$ (pH = 6.8)	scanned from −1.01 V to 1.3 V versus NHE and back at 50 mV/s every 15 min				1 h	-	restoration of catalytic activity	inhibition of poisoning and restructuring	Kedzierzawski and Augustynski[39]
Cu (0.28 cm^2)	0.1 M $NaHCO_3$ or 0.5 M $KHCO_3$	3 scans every 5 min from −1.72 to +1.3 V versus NHE at 5 V/s				50 h	CH_4 ~ 10%, C_2H_4 ~ 25%	maintained high hydrocarbon selectivity over long times	surface oxidation and roughening	Jermann and Augustynski[21]
Ag (0.65 cm^2)	0.1 M $KHCO_3$	$-2.5\ V \leq E_c \leq -1.75$ V versus Ag/AgCl	5 s	$-0.8\ V \leq E_a \leq -0.1$ V versus Ag/AgCl	5 s	10 h	H_2 ~ 10%, CO ~ 70%, C_2H_5OH ~ 22%, CH_4 ~ 55%, C_2H_4 ~ 3%	selectively tune hydrocarbon formation	rearrangement of surface coverage (specifically of H_{ad})	Shiratsuchi and Nogami[38]
Cu (1 cm^2)	0.5 M $KHCO_3$ (pH = 7.3)	−2.2 V versus SHE	50 s	0.05 V versus SHE	10 s	0.5 h	-	recovered electrode activity	inhibition of poisoning	Friebe et al.[40]

(Continued on next page)

https://doi.org/10.1016/j.joule.2021.05.014

Table 1. Continued

Catalyst	Electrolyte[a]	Anodic treatment				Stability	Selectivity[b]	Effect of anodic treatment	Hypothesis	Ref.
		E_a, I_a	t_a	E_a, I_a	t_a					
Cu/Ag alloy	0.1 M $KHCO_3$	$-2.5\ V \leq E_a \leq -1.9\ V$ versus Ag/AgCl	5 s	0.25 V ≤ E_a ≤ 0.9 V versus Ag/AgCl	5 s	8 h	-	selective production of C_2 products, tune C_2 FE by varying alloy ratio	surface oxidation on Cu, rearrangement of surface coverage on Ag (specifically of CO_{ad})	Ishimaru et al.[39]
Cu (0.2 cm^2)	0.1 M $KHCO_3$ (pH = 6.5)	−2.1 V versus SCE	10 s	0 V versus SCE	5 s	7.5 h	-	prevented graphitic deposition and observed stable methane production	inhibition of poisoning and surface oxidation	Lee and Tak[41]
Cu and Cu oxide (mixture of Cu_2O and CuO)	0.1 M $KHCO_3$	$-4\ V \leq E_a \leq -1$ V versus Ag/AgCl	3 s	0 V ≤ E_a ≤ 2 V on Cu and −4 V ≤ E_a ≤ −0.5V on Cu oxide	1–9 s	1 h	H_2 ~ 10%, CH_4 ~ 50%, C_2H_4 ~ 30%	enhanced ethylene selectivity by varying anodic potential, even more ethylene observed on copper oxide electrode	inhibition of poisoning and surface oxidation	Yano and Yamasaki[42]
Cu	0.1 M $KHCO_3$	50 A/m^2	5 s	0 A/m^2	5 s	-	-	pulsing maintains a higher average CO_2 concentration at the surface, predicted pH varies over a range of 1.5 units during pulsing	enhanced CO_2 concentration at the cathode	Gupta et al.[40,b]
Cu (3.14 cm^2)	0.2 M $KHCO_3$ (pH = 7)	galvanostatic reduction (−5 mA/cm^2) with 3 CV scans (−1.2 to −0.1 V versus Ag/AgCl, 100 mV/s) every 15 min, 1, 2, and 5 h or with potential steps to −0.25, −0.5, −1.2 V versus Ag/AgCl for 84s every 2 h				10 h	H_2 ~ 40%, CO ~ 50%, CH_4 ~ 50%, C_2H_4 ~ 6%	frequent CV scans reduced CO_2R activity, short steps to mild cathodic potentials favored CO at the expense of CH_4	rearrangement of surface coverage (specifically of H_{ad} and CO_{ad})	Lim et al.[51]

(Continued on next page)

https://doi.org/10.1016/j.joule.2021.05.014

Table 1. Continued

Catalyst	Electrolyte[a]	Anodic treatment				Stability	Selectivity[b]	Effect of anodic treatment	Hypothesis	Ref.
		E_a, I_a	t_a	E_a, I_a	t_a					
Cu-DHP (4.29 cm^2)	0.1 M $KHCO_3$	−1.8 V ≤ E_a ≤ −1.5V versus Ag/AgCl	5–500 s	−0.88 V ≤ E_a ≤ 0.15V versus Ag/AgCl	5 s	95 h	H_2 ~ 10%, CH_4 ~ 10%, C_2H_4 ~ 35%	constant HER suppression and stable hydrocarbon formation over long times	surface oxidation and reconstruction	Engelbrecht et al.[50]
Pb (0.81 cm^2)	1 M $KHCO_3$	−1.1 V versus RHE	0.002 s ≤ t_a + t_c ≤ 10 s	0.1 V versus RHE	0.002 s ≤ t_a + t_c ≤ 10 s	16 h	$HCOO^-$ ~ 50%	highly stable and enhanced formate production	surface oxidation	Biom et al.[50]
$Pd_{0.6}Ag_{99}/C$ (0.5 cm^2)	0.5 M $NaHCO_3$	−0.8 V versus RHE	590 s	1.22 V versus RHE	10 s	45 h	$HCOO^-$ ~ 98%	observed stable formate production for 45 h	inhibition of poisoning	Lee et al.[33]
Cu and Cu(100) (0.79 cm^2)	0.1 M $KHCO_3$	−1 V versus RHE	0.2 s ≤ t_c ≤ 1 s	0 V ≤ E_a ≤ 0.8 V versus RHE	1 s	1 h	C_2H_5OH + C_2H_4 + C_3H_7OH ~ 76%	observe enhanced C_{2+} formation with the presence of (100) terraces, Cu_2O, and defects on Cu(100)	surface oxidation	Arán-Ais et al.[52]
Mixed-valence OD-Cu nanocubes (0.78 cm^2)	0.5 M $KHCO_3$ (pH = 7.2)	−1.15V ≤ E_c ≤ −0.7 V versus RHE	10 s	0.5 V versus RHE	10 s	1 h	C_2H_5OH ~ 13%	exclusively produce ethanol as the only CO_2R product, maintain ratio of half-Cu^0 to half-Cu^+ throughout the entire experiment	surface oxidation and rearrangement of surface coverage (specifically of OH species at the Cu^0/Cu^+ boundary)	Lin et al.[53]
Cu_2- Cu_2O_{-x} and Cu_2O GDE	1 M KOH	two treatments: apply −2.2 V versus Ag/AgCl for 1 h, (1) hold at 1.5 or 0.1 V versus Ag/AgCl for 5 min, (2) scan from −1.1 V to −0.5V versus Ag/AgCl at 50 mV/s for 20 cycles				6 h	H_2 ~ 40%, C_2H_4 ~ 28%	restored cell performance and surpassed original cell activity using anodic treatment	surface reconstruction	Lee et al.[34,c]

(Continued on next page)

https://doi.org/10.1016/j.joule.2021.05.014

Table 1. Continued

Catalyst	Electrolyte[a]	Anodic treatment				Stability	Selectivity[b]	Effect of anodic treatment	Hypothesis	Ref.
		E_c, i_c	t_c	E_a, i_a	t_a					
Ag	0.1 M of K_2CO_3 + x M of EMISE ionic liquid (x = 0.1) (pH = 7.2)	−1.4 V, −1.5V, and −1.6 V versus Ag/AgCl	5 s	0 V versus Ag/AgCl	5 s	0.5 h	H_2 ~ 11%, CO ~ 73%	enhance CO formation and suppress HER	enhanced CO_2 concentration at the cathode	Oguma and Azumi[35]
Cu (0.5 cm^2)	0.05 M Cs_2CO_3	−1.15V versus RHE	5, 10, 25 s	−0.8 V versus RHE	5, 10, 60 s	0.5 h	H_2 ~ 11%, C_{2+} ~ 81%	HER suppression and enhancement in C_{2+} formation	reamangement of surface coverage (specifically CO_{ads}/H_{ads}) and enhanced CO_2 concentration at the cathode	Kim et al.[36]
Cu-DHP (10 cm^2)	0.1 M $KHCO_3$	−1.38 V versus Ag/AgCl	25 s	−1 V versus Ag/AgCl	5 s	16 h	C_2H_4 ~ 23%	demonstrated stable ethylene formation for over 16 h in a flow cell, recovered catalytic activity of a deactivated electrode using anodic pulses	suspected reconstruction	Jannsch et al.[37]
Ag and Cu GDE	MEA electrolyzer (0.1 M $KHCO_3$ anolyte)	−3.6 V (full MEA cell voltage)	60 s	−2 V (full MEA cell voltage)	30 s	226 h	On Cu: C_2 ~ 80% On Ag: CO ~ 90%	no detectable cell-damaging carbonate salt formation and no degradation in performance	regeneration period halts hydrocarbon formation while maintaining electric field for carbonate ions to migrate to the anode	Xu et al.[34]
Cu	0.1 M $CsHCO_3$	−1.85V ≤ E_c ≤ −1.55V versus RHE	5-20 s	−1.3 V ≤ E_a ≤ −0.85V versus RHE	5-20 s	-	C_{2+} ~ 65%	enhancement of C_{2+} FE under pulsed conditions	enhanced transient CO_2 concentration and heightened pH near the cathode	Bui et al.[35b]

(Continued on next page)

Table 1. Continued

Catalyst	Electrolyte[a]	Anodic treatment				Stability	Selectivity[b]	Effect of anodic treatment	Hypothesis	Ref.
		E_a, I_a	t_c	E_a, I_a	t_a					
Cu_2O Nanocubes GDE	1 M KOH (pH = 13.7)	−0.7 V versus RHE	1 s	0.6 V ≤ E_a ≤ 1.5V versus RHE	1 s	10 h	C_2H_4 ~ 44%, C_2H_5OH ~ 20%, CH_4 ~ 48%	observed 10% enhancement of C_2 FE when E_a = 0.9 V and high CH_4 selectivity when E_a = 1.2 V	surface reconstruction and changes in local pH	Jeon et al.[96]

[a]Electrode geometric surface area and pH of CO_2-saturated electrolyte included in tabulated information when provided in publication
[b]Indicates results are based on numerical calculations and not experimental observations
[c]Indicates that data refers to CO reduction (as opposed to CO_2 reduction)

Please cite this article in press as: Casebolt et al., Pulse check: Potential opportunities in pulsed electrochemical CO_2 reduction, Joule (2021), https://doi.org/10.1016/j.joule.2021.05.014

Table 2. "Short" pulses (<1 s)

		Anodic treatment								
Catalyst[a]	Electrolyte[a]	E_c	t_c	E_a	t_a	Stability	Selectivity[b]	Effect	Hypothesis	Ref.
Cu (5 cm^2)	0.1 M $KHCO_3$ (pH = 6.8)	−1.05 V, −1 V, and −0.95V versus RHE	10 ms ≤ t_c ≤ 100 ms	0.6 V versus RHE	10 ms ≤ t_a ≤ 150 ms	1 h	H_2 ~ 97%, CO ~ 64% (optimizing syngas formation, so reporting highest H_2 FE)	exclusively form H_2 and CO, molar ratio of H_2:CO is pulse time dependent	surface oxidation, and rearrangement of surface coverage/ shifting EDL changes interfacial energetics	Kumar et al.[46]
Cu(100) and Cu(111)	phosphate buffer solution (pH = 7.9)	−0.8 V versus RHE	50 ms, 100 ms	−0.35V ≤ E_a ≤ −0.2 V versus RHE	50 ms, 100 ms	1 h	-	pulse voltammetry guarantees reproducible initial conditions, formed significantly more oxygenated hydrocarbons under alternating voltage conditions	rearrangement of surface coverage (specifically OH_{ads})	Le Duff et al.[47]
Cu (0.1 cm^2)	0.1 M $KHCO_3$ (pH = 6.8)	−1.2 V ≤ E_c ≤ −0.85V versus RHE	50 ms – 1 s	0.6 V versus RHE	50 ms – 1 s	2 h	H_2 ~ 5%, CH_4 ~ 75%, CO ~ 50%	HER suppression and enhanced CO_2R selectivity and activity	rearrangement of surface coverage (specifically of H_{ads})	Kimura et al.[44]
OD-Cu (3 cm^2)	0.1 M KOH (pH = 13)	−0.35V versus RHE	10 ms – 50 s	0 V versus RHE	10 ms – 50 s	1 h	H_2 ~ 29%, CH_4 ~ 60%, $HCOO^-$ ~ 30%	favor CO reduction over HER, increased selectivity for single-carbon products when pulse frequency < 1 s	rearrangement of surface coverage/ shifting EDL changes interfacial energetics	Strain et al.[49,c]
Cu (0.2 cm^2)	0.1 M $KHCO_3$ (pH = 6.8)	−1.15V ≤ E_c ≤ −0.8 V versus RHE	50 ms	−0.8 V ≤ E_a ≤ 0.6 V versus RHE	50 ms	4 h	H_2 ~ 10%, CO_2R ~ 90%	pulsing suppresses HER in CO and CO_2 reduction, Cu remains metallic over wide range of pulse profiles and only form $Cu(OH)_2$ in the bulk when E_a > +0.6 V versus RHE	rearrangement of surface coverage (specifically H_{ads} and OH_{ads})	Kimura et al.[45]

(Continued on next page)

used to drive the reaction are usually high. Coupled with the low solubility of CO_2 in aqueous solutions, the rapid consumption of CO_2 at the surface can result in CO_2 diffusion being the rate limiting process.

Understanding the spatiotemporal concentration profiles within the boundary layer during p-eCO_2R presents an interesting challenge and opportunity since the CO_2 depleted at the electrode surface during the cathodic "on" pulse can be replenished during the anodic "off" pulse. The extent to which the CO_2 levels within the boundary layer are replenished can be estimated with mathematical models as was shown by Gupta et al.[43] The optimal "off" pulse duration is governed by the balance of two factors: (1) long enough "off" pulse to substantially replenish CO_2 levels but (2) not too long that the production time is lost within the cycle period. Kim et al. recently reported a synergistic integration of experiment and computation to show how this replenishing effect enhances p-eCO_2R performance toward C_{2+} product formation.[5,6]

The boundary layer thickness is a key consideration in the analysis of mass transport effects. In the case of p-eCO_2R, thicker boundary layers require longer "off" pulse durations to replenish CO_2 levels. For a typical boundary layer thickness of about 100 μm, an "off" pulse duration of 5–10 s is required,[43,56] indicating that in studies with longer pulse profiles, enhanced mass transport of CO_2 to the surface is a relevant consideration in explaining the pulse mechanism. However, when the pulse profile is on the order of milliseconds, there is no significant change in [CO_2] at the surface, meaning that the pulse-dependent product selectivity observed in millisecond p-eCO_2R experiments is therefore not due to the replenishing effect.[44,46,48]

To tune into the replenishing effect for millisecond pulse profiles, one can reduce the boundary layer thickness from the electrode. With thinner boundary layers due to improved mass transport (e.g., rotating disk electrodes or GDEs), the replenishing effect can be accomplished with much shorter "off" pulses. Complementary computational models (taking into account CO_2 diffusion and CO_2 reaction in the bicarbonate buffer equilibrium and CO_2 reduction reactions, Figure 3C) provide valuable insight into the effectiveness of the replenishing effect by illustrating the relationship between boundary layer thickness and "off" pulse duration, as shown in Figures 3A and 3B (unpublished simulations based on the reaction-diffusion model developed by Gupta et al.[43]). In the case of a 100-μm thick boundary layer, 50 ms is not long enough to significantly replenish the concentration of CO_2 at the surface, whereas in the case of a 50-μm thick boundary layer, 50 ms is a long enough "off" pulse to restore [CO_2] at the interface to near its initial condition.

To investigate the effects of heightened CO_2 concentration at the surface due to enhanced mass transfer during the "off" pulse under millisecond pulse profile conditions, Kimura et al. tested the resulting selectivity of static versus pulsed electrolysis in enhanced mass transport experiments. Using facilitated convection at a planar electrode where 1,000 rpm corresponded to a boundary layer of ~10 μm, 50 ms pulses were long enough to replenish [CO_2] at the surface (Figure 3B).[44] If the pulse mechanism operates by improved mass transport alone, then the stirred static potential experiment should have the same effect as the non-stirred pulsed potential experiment. However, as seen in Figure 3D, pulsing significantly suppresses hydrogen formation, and the resulting product selectivities between the pulsed and static experiments look very different.[44] Further, if pulsing works solely by improved mass transport effects, then going from pulsed non-stirred to pulsed stirred should not experience any changes in selectivity, rather just a uniform

Please cite this article in press as: Casebolt et al., Pulse check: Potential opportunities in pulsed electrochemical CO_2 reduction, Joule (2021), https://doi.org/10.1016/j.joule.2021.05.014

Table 2. Continued

Catalyst[a]	Electrolyte[a]	Anodic treatment E_c	Anodic treatment t_c	E_a	t_a	Stability	Selectivity[b]	Effect	Hypothesis	Ref.
Cu (0.1 cm^2)	$KHCO_3$ and KCl at varying concentrations	−1.05V versus RHE	50 ms	0.4 V versus RHE	50 ms	24 h	In $KHCO_3$: CH_4 ~ 40%, CO ~ 70% In KCl: C_2 ~ 70%	pulsing maintains high CO_2R selectivity and activity over 24 h, increasing $[KHCO_3]$ increased CH_4 selectivity, increasing [KCl] increased C_2 product selectivity, HER suppressed under all conditions	rearrangement of surface coverage (specifically OH_{ads}, H_{ads}, and CO_{2ads}), as well as presence (or lack thereof) of facile proton donors (HCO_3^-)	Casebolt et al.[45]
Cu (0.3 cm^2)	0.1 M $KHCO_3$	−1.15 V ≤ E_c ≤ −0.9 V versus RHE	100 ms – 1 s	0.6 V versus RHE	100 ms – 1 s	6 h	5°C: C_2H_5OH ~ 40%, C_2H_4 ~ 10%, H_2 ~ 10% 25°C: C_2H_4 ~ 67%, C_2H_5OH ~ 10%, H_2 ~ 10%	higher temperatures favor ethylene and lower temperatures favor ethanol. The ratio of ethanol to ethylene increases with increasing time constant (aka decreasing temperature)	rearrangement of surface coverage (specifically H_{ads} and CO_{2ads}) and temperature control to stabilize Cu^+ species	Tang et al.[97]

●● Lowest observed H_2 selectivity and highest observed CO_2RR or CORR product selectivity reported (this means that reported values are not necessarily from the same pulse conditions)
EMSE, 1-ethyl-3-methylimidazolium ethylsulfate; EDL, electrochemical double layer; GDE, gas diffusion electrode; OD-Cu, oxide-derived copper; DHP, deoxidized high phosphorous copper
[a]Electrode geometric surface area and pH of CO_2-saturated electrolyte included in tabulated information when provided in publication
[b]Indicates results are based on numerical calculations and not experimental observations
[c]Indicates that data refers to CO reduction (as opposed to CO_2 reduction)

JOULE 993

used to drive the reaction are usually high. Coupled with the low solubility of CO_2 in aqueous solutions, the rapid consumption of CO_2 at the surface can result in CO_2 diffusion being the rate limiting process.

Understanding the spatiotemporal concentration profiles within the boundary layer during p-eCO_2R presents an interesting challenge and opportunity since the CO_2 depleted at the electrode surface during the cathodic "on" pulse can be replenished during the anodic "off" pulse. The extent to which the CO_2 levels within the boundary layer are replenished can be estimated with mathematical models as was shown by Gupta et al.[43] The optimal "off" pulse duration is governed by the balance of two factors: (1) long enough "off" pulse to substantially replenish CO_2 levels but (2) not too long that the production time is lost within the cycle period. Kim et al. recently reported a synergistic integration of experiment and computation to show how this replenishing effect enhances p-eCO_2R performance toward C_{2+} product formation.[5,6]

The boundary layer thickness is a key consideration in the analysis of mass transport effects. In the case of p-eCO_2R, thicker boundary layers require longer "off" pulse durations to replenish CO_2 levels. For a typical boundary layer thickness of about 100 μm, an "off" pulse duration of 5–10 s is required,[43,56] indicating that in studies with longer pulse profiles, enhanced mass transport of CO_2 to the surface is a relevant consideration in explaining the pulse mechanism. However, when the pulse profile is on the order of milliseconds, there is no significant change in [CO_2] at the surface, meaning that the pulse-dependent product selectivity observed in millisecond p-eCO_2R experiments is therefore not due to the replenishing effect.[44,46,48]

To tune into the replenishing effect for millisecond pulse profiles, one can reduce the boundary layer thickness from the electrode. With thinner boundary layers due to improved mass transport (e.g., rotating disk electrodes or GDEs), the replenishing effect can be accomplished with much shorter "off" pulses. Complementary computational models (taking into account CO_2 diffusion and CO_2 reaction in the bicarbonate buffer equilibrium and CO_2 reduction reactions, Figure 3C) provide valuable insight into the effectiveness of the replenishing effect by illustrating the relationship between boundary layer thickness and "off" pulse duration, as shown in Figures 3A and 3B (unpublished simulations based on the reaction-diffusion model developed by Gupta et al.[43]). In the case of a 100-μm thick boundary layer, 50 ms is not long enough to significantly replenish the concentration of CO_2 at the surface, whereas in the case of a 50-μm thick boundary layer, 50 ms is a long enough "off" pulse to restore [CO_2] at the interface to near its initial condition.

To investigate the effects of heightened CO_2 concentration at the surface due to enhanced mass transfer during the "off" pulse under millisecond pulse profile conditions, Kimura et al. tested the resulting selectivity of static versus pulsed electrolysis in enhanced mass transport experiments. Using facilitated convection at a planar electrode where 1,000 rpm corresponded to a boundary layer of ~10 μm, 50 ms pulses were long enough to replenish [CO_2] at the surface (Figure 3B).[44] If the pulse mechanism operates by improved mass transport alone, then the stirred static potential experiment should have the same effect as the non-stirred pulsed potential experiment. However, as seen in Figure 3D, pulsing significantly suppresses hydrogen formation, and the resulting product selectivities between the pulsed and static experiments look very different.[44] Further, if pulsing works solely by improved mass transport effects, then going from pulsed non-stirred to pulsed stirred should not experience any changes in selectivity, rather just a uniform

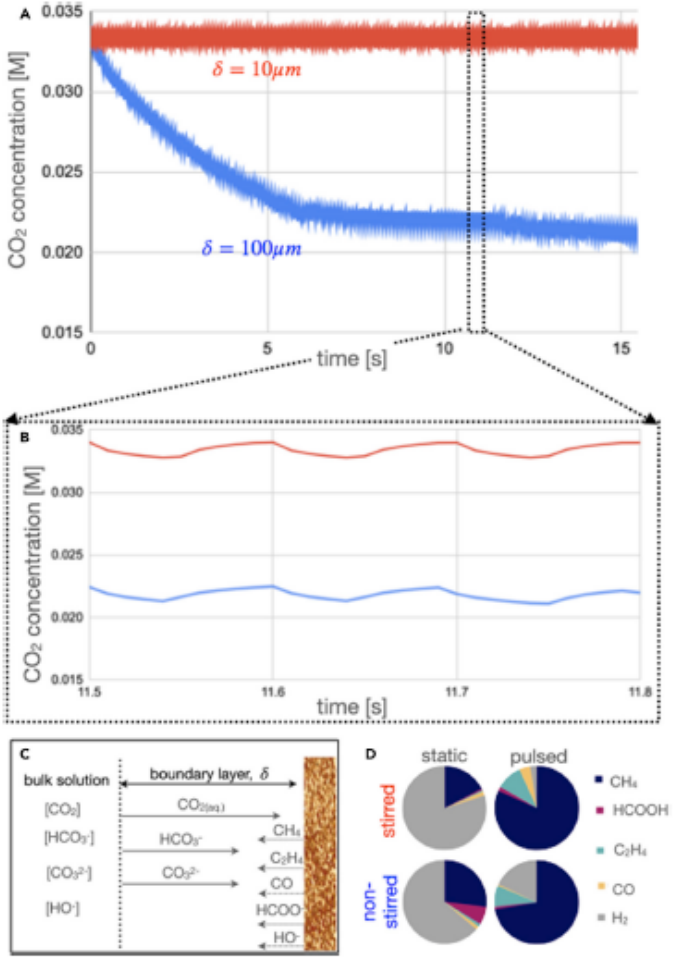

Figure 3. Boundary layer effects on product selectivity in pulsed- and constant-potential electrochemical CO_2 reduction

(A and B) Modeled CO_2 surface concentration for thin (10 μm) and thick (100 μm) boundary layer thickness [unpublished] based on equations developed in Gupta et al.,[43] Thinner boundary layer enables faster replenishing of CO_2 during short (50 ms) pulse times.

(C) Illustration of coupled transport and reaction equilibria of key species within the boundary layer near the electrode surface.

(D) experimental faradic efficiency for pulsed- and constant-potential CO_2 reduction in thick and thin boundary layers from Kimura et al.,[44] Pulsed: $E_c = -1.2$ V, $E_a = +0.6$ V versus RHE, $t_a = t_c = 50$ ms. Static: E = −1.2 V versus RHE. Stirred at 1,000 rpm.

increase in current density (since faster mass transport of reactants to the surface results in faster reaction rates). However, as seen in Figure 3D, in pulsed experiments going from unstirred to stirred, methane selectivity increases. These discrepancies mean that changes in mass transport conditions alone are unable to explain the

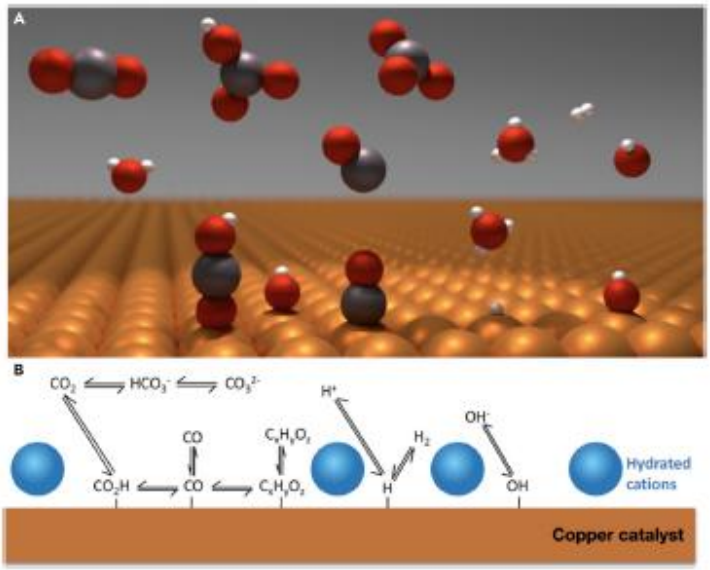

Figure 4. Understanding surface adsorbate coverage in dynamic interfacial environment
(A) illustrative rendering of reaction environment including key eCO_2R participants on Cu.(100)
(B) Simplified schematic of relevant species and equilibrated processes in the EDL.

observed trends in product selectivity under short pulse conditions. The interdependent effects of thermodynamics, kinetics, and mass transport make it impossible to definitively rule out any one process, but based on the discussion above, we suggest that improvements in mass transport are not a major contributor to the trends observed during millisecond pulse conditions.

Switching gears back to longer pulse profiles, another recent study investigating the effects of pulsing on CO_2 concentration at the surface by Bui et al., modeled the effects of pH and CO_2 concentration on the kinetics for forming individual products for pulse times ranging from 5 to 20 s.[95] Similar to previous studies, they too found that enhanced CO_2 concentration at the surface is not solely responsible for enhanced C_{2+} product selectivity under pulsed conditions. Instead, they found enhanced C_{2+} product selectivity is due to a combination of factors driven by repeatedly accessing a transient state of high pH, CO_2 concentration, and overpotential during p-eCO_2R.

From these studies we observe that pulsing can affect the CO_2 concentration at the surface depending on the pulse duration and boundary layer thickness, but that CO_2 concentration alone is not enough to explain the trends observed under p-eCO_2R.

Surface adsorbate coverage and dynamics

Moving from mass transport through the boundary layer to the adsorbates on the surface of the electrode, an abrupt switching of the applied potential can significantly rearrange the EDL and the interfacial adsorbate coverage. Since charged species respond to variations in electrode polarity, each pulse is expected to modulate the coverage of ions, including H^+/H_3O^+, OH^-, electrolyte ions, and also critical reaction intermediates (like *CO–CO and *CO–CHO) due to their large dipole moments[26] (Figure 4).

Please cite this article in press as: Casebolt et al., Pulse check: Potential opportunities in pulsed electrochemical CO_2 reduction, Joule (2021), https://doi.org/10.1016/j.joule.2021.05.014

CO reduction (COR) experiments provide important insight into the reaction mechanism as well as specific insight into the role of surface-adsorbed species. The observed COR product enhancements and HER suppression reported by Strain et al. under pulsed conditions were attributed to dynamic interfacial chemistry. Specifically, they argued that the non-faradic current during the charging/discharging (regime I, Figure 1C) dominates short pulses in the millisecond regime, which modifies the binding energy and species adsorption, acting to inhibit HER.[49] Similarly, Arán-Ais et al. noted that the positive polarization of the electrode during pulsing lowers the surface hydrogen coverage, and that higher OH_{ads} coverage is expected with increasing E_a.[52] In one set of experiments, they observed improved ethanol selectivity when E_a = 0 V versus RHE, where minimal Cu^+ coverage was measured and only minor surface rearrangement was observed. They attributed this selectivity observation to higher OH_{ads} coverage as a result of the anodic pulse.[52]

There is an emerging consensus that the dynamic surface coverages of hydrogen (H_{ads}) and hydroxide (OH_{ads}) play a critical role in the p-eCO_2R mechanism. Shiratsuchi et al. in 1996 pointed out the importance of local proton concentration, ascribing selectivity differences to the extent of surface coverage of adsorbed hydrogen which can be controlled by the anodic bias.[38] When the anodic potential was more negative than −0.4 V versus Ag/AgCl, the increase in local proton concentration at the surface resulted in the formation of CH_4, C_2H_4, and C_2H_5OH, while when the potential was less negative, desorption of adsorbed hydrogen occurred resulting in preferential production of less protonated products (i.e., CO and HCOOH).[38] Le Duff et al. proposed that the shift toward the production of oxygenated hydrocarbons under pulsed conditions occurs as a result of decreased H_2 availability and increased OH_{ads} surface coverage during p-eCO_2R.[47] DFT calculations support this interpretation, finding that the presence of hydroxides on copper surfaces lowers the binding energy of CO while also stabilizing the OCCO intermediate through dipole interactions, thereby lowering the activation barrier for the CO dimerization step.[102]

Time-resolved vibrational spectroscopy provides helpful clues to better understand the dynamic surface coverage of reaction intermediates. In a surface-enhanced infrared absorption spectroscopy (SEIRAS) study tracking CO_{atop} and CO_{bridge} species over time as a function of potential, Chou et al. found that CO_{atop} formation on copper is a dynamic adsorption process.[103] Their data suggested that CO_{bridge} can be removed from the copper surface during the copper oxidation. Similarly, Gunathunge et al. found that CO_{atop} converts to an irreversibly adsorbed, inactive CO_{bridge} species during cathodic polarization in alkaline conditions when the total CO coverage is lowered below the saturation coverage, and that this species can only be removed by oxidizing the copper.[104] A study by Iijima et al. found that the presence of adsorbed hydroxides promotes CO adsorption and prevents the eventual deactivation by irreversibly bound CO_{bridge} species through a near neighbor coupling effect.[100]

Kimura et al. postulated that the anodic pulse displaced H_{ads}[44] and promoted OH_{ads} formation.[46] This OH_{ads} adsorption promotes the CO_{atop} binding while preventing the CO_{atop} from transforming into the inactive CO_{bridge} species.[100] CO adsorption competes with H adsorption,[105] so the enhanced presence of bound CO significantly suppresses HER.[106] Kim et al. also suggests that pulsing enhances the surface concentrations of adsorbed CO versus H, which results in increased C_{2+} selectivity and HER suppression.[56] Variations in surface coverage are an important consideration because deviations from the thermodynamic coverage of different intermediates could drastically change product selectivity and reactivity. In the work by Lim

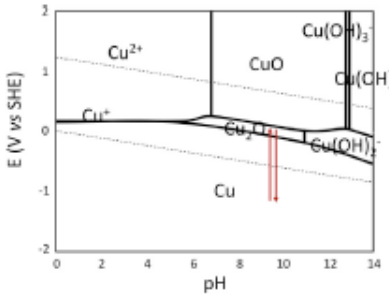

Figure 5. Pourbaix diagram
Identification of thermodynamically stable copper species at a given pH and potential (V versus SHE) at 25°C and $[Cu(aq)]_{sol.} = 10^{-6}$ mol/kg. Dotted lines indicate water stability window and red arrows demonstrate possible phase change. Beverskog and Puigdomenech.[107]

et al.,[51] a potential step treatment (up to −1.2 V versus Ag/AgCl) applied every two hours improved CO formation at the expense of methane. They proposed that there are multiple steady states for surface coverage (enabled by competitive adsorption between H and CO) that they could switch between. Collectively, these studies add to the growing body of evidence that the product selectivity of p-eCO_2R results from a mechanism based on the concerted interplay between dynamic changes in surface adsorbates, improved CO_2 transport (*vide supra*), and changes in catalyst composition and structure (*vide infra*).

Copper oxide formation

A Pourbaix diagram provides a useful description for the dynamic changes in the electrode composition (i.e., oxidation state, see Figure 5).[107] Depending on the combination of applied potential and pH, copper can exist in a variety of oxidation states. The Pourbaix diagram describes the phase at equilibrium. However, since the p-eCO_2R involves a choreography of several non-equilibrium processes, the key question is how the kinetics of the conversion between these equilibria compares to the kinetics (i.e., pulse profile) of the applied pulse.

The first pulsing studies on copper hypothesized that pulsing created different surface conditions compared with constant-potential reduction. The proposed mechanism was that during the anodic pulse the surface is oxidized to Cu_2O which favors intermediate adsorption; these findings were corroborated with *ex situ* XPS and XRD.[30,36,41] Insights from *in situ* studies of the time-resolved electrode composition, especially in the case of oxide-derived copper (OD-Cu) can provide important clues to understand the related mechanism in p-eCO_2R considering the hypothesized copper oxide formation and subsequent reduction.

While eCO_2R is carried out at strongly cathodic potentials, some researchers suggested and observed $O_{(s)}$ and/or Cu^+ species to persist at the surface/subsurface during the eCO_2R on pulsed copper and OD-Cu catalysts.[31,108–115] However, these findings are subject to an ongoing debate with several computational and experimental studies which showed that the presence of oxygen species is highly unlikely and that copper is fully reduced prior to CO_2 reduction, identifying Cu^0 as the active species.[26,54,94,102,104,116–126] Several groups have suggested observations of residual oxygen are due to the copper oxidation in air during sample transfer, complicating the experimental analysis of the Cu oxidation state.[118,127,128] Chang et al. showed that Cu^0 can spontaneously reoxidize to Cu^+ in aqueous electrolyte (verified using *in situ* Raman spectroscopy and *in situ* XAS), and showed that this reaction occurred simultaneously with the eCO_2R.[128] Similarly, *in situ* GIXAS and GIXRD

data from Lee et al. showed that after releasing the applied potential, Cu_2O was detected in the bulk within 5 min, demonstrating that metallic copper can easily reoxidize at the OCP even without exposure to ambient conditions.[54] These findings highlight the ease of copper oxidation when extracting the sample for *ex situ* characterization or when removing the applied potential. Since there is no guarantee that the copper oxidation states reported in *ex situ* characterization studies or in characterization studies that are not conducted under relevant operating conditions actually exist during reaction, we caution the reader against drawing definitive conclusions from *ex situ* findings. Nonetheless, even with the *in situ*/vacuum-transfer investigations of OD-Cu and pulsed copper, observations of Cu^+ have been reported throughout electrolysis.[52,128] These diverging observations of the heavily debated topic of copper oxidation further emphasize the importance and need for using *operando* techniques to explore the catalyst surface during reaction for real-time insight into what the catalyst looks like under operating conditions.

Beyond the open question regarding the presence of Cu^+ sites during eCO_2R,[129] there are also ongoing debates concerning the mechanistic role of Cu^+ to enhancing catalytic activity and reaction selectivity with proposed effects ranging from increased ECSA to stronger binding sites or increased occurrence of grain boundaries and other defects.[5] It has been suggested that copper oxide formation results in surfaces with a high density of grain boundaries,[130] where the density of grain boundaries has been directly correlated to enhanced CO reduction activity and selectivity.[131] Contrarily, other studies postulate that it is instead an effect of increased ECSA, which increases geometric reaction rates and creates a higher local pH environment thereby favoring C_{2+} products.[132] Other studies argue that beyond increased grain boundaries and roughness, OD-Cu electrodes experience stronger intrinsic CO binding. An *in situ* ATR-SEIRAS study by Lee et al. showed that CO binds more strongly on the surface of copper oxides than on pure copper.[133] Increased CO binding and coverage correlates to the increased C_2 product formation, since the formation rates of the C_{2+} products have a second-order dependence on CO_{ads} coverage.[5,56,134] A DFT study by Liu et al. showed that the presence of subsurface oxygen on disordered OD-Cu increases the maximum adsorption coverage of CO,[135] and further, it has been suggested that copper oxides favor C_2 formation by preventing the adsorbed CO from being protonated.[93] However, a study by Ren et al. found that they could achieve 40% methane selectivity on a CuO-film, challenging claims that the presence of copper oxide species is the most crucial factor in determining selectivity between C_1 and C_{2+} products.[123] We note that there remain outstanding questions with regards to the presence of Cu^+ in the bulk versus on the electrocatalytically active surface. Further complicating our understanding of the effects of Cu^+, is a study by Chen et al. that used *in situ* SERS to show an inverse correlation between the presence of a Cu_2O layer and CO and C_2 production, suggesting that removing Cu_2O results in more active Cu sties for CO adsorption.[136] Other models have found that it is actually the combination of Cu^0 and Cu^+ sites that enhances C_{2+} production. Some models have demonstrated that C–C coupling is favorable on surfaces with a mix of Cu^0 and Cu^+ surface sites,[137] while others suggest that the interatomic bond distance between the Cu atoms on Cu_2O surfaces is too large for C–C coupling to be likely.[128] We do not try to establish the basis of OD-Cu activity here, rather we aim to present relevant information that supplements our understanding of how the pulse mechanism operates. Pulse studies will likely not be able to settle these debates outright. Instead, pulsing provides an opportunity to collect complementary data for the observation and effects of oxides because while the presence of copper oxides on OD-Cu and the role of Cu^+ under potentiostatic eCO_2R is not agreed upon, p-eCO_2R often involves anodic potentials for which

Please cite this article in press as: Casebolt et al., Pulse check: Potential opportunities in pulsed electrochemical CO_2 reduction, Joule (2021), https://doi.org/10.1016/j.joule.2021.05.014

the formation of oxide species is thermodynamically expected. How rapidly these oxides form relative to the pulsed applied potential remains an outstanding question that will hopefully be resolved by future *in situ* and *operando* experiments.

A recent p-eCO_2R study by Arán-Ais et al. used vacuum-transfer Auger electron spectroscopy to examine the nature of Cu during the p-eCO_2R reaction.[52] Their experiments focused on pulsing on single crystal Cu(100) ($E_c = -1$ V, $0 \leq E_a \leq 0.8$ V versus RHE, $t_a = t_c = 1$ s), where they uncovered that Cu^+ sites form during the anodic pulse proportional to E_a, and that these sites persist during the cathodic pulse.[52] When $E_a = 0.4$ V, they measured 14% of surface species to be Cu_2O, and 4% remained during cathodic pulse at −1 V versus RHE. When testing a Cu(100) electrode with the same defect density but different Cu^+ content, Arán-Ais observed higher ethanol selectivity when the cathodic time was shorter, meaning there was more Cu^+ remaining on the surface.[52] They observed a clear increase in the ethanol selectivity when Cu^0 and Cu^+ coexisted. This observation supports the hypothesis that the concurrence of Cu^+ and Cu^0 species enhances the CO dimerization.[103,137] Like Arán-Ais, Lin et al., highlights the importance of Cu^+ species in the ethanol formation, demonstrating that a pulsed-potential program ($E_a = 0.5$ V, $-1.15 \leq E_c \leq -0.7$ V versus RHE, $t_a = t_c = 10$ s) can maintain the existence of Cu^+ species throughout electrolysis using *operando* time-resolved XAS.[53] Their DFT studies also suggested that the co-existence of Cu^+ and Cu^0 sites encourages C_2 product formation through a carbonyl stabilization mechanism. *Operando* SERS data by Jeon et al. also imply that Cu^+ and Cu^0 sites coexist on the catalyst surface during pulsed electrolysis.[96] DFT studies by De Luna et al. suggest that Cu^+ plays a crucial role in shifting the product distribution toward C_2 products rather than C_1, in line with their experimental observations using *in situ* XAS.[138] The co-existence of these copper sites is suggested to enhance CO dimerization because of differences in the CO binding. Chou et al. observed that CO_{atop} forms on Cu^+, while CO_{bridge} forms on Cu^0, and when both Cu^+ and Cu^0 were observed, they measured an enhancement in ethylene selectivity.[103] A recent study by Tang et al. offers some additional insight into discrepancies observed around the effects of Cu^+ and which C_2 product it enhances.[97] Conducting temperature-controlled experiments between 5°C–25°C, Tang et al. found that ethylene is favored at higher temperatures, while ethanol is favored at lower temperatures. These observations coincided with observations of a larger system RC time constant with decreased temperature, where the response time is the time in which the initial sharp current spike decays to a stable current after a potential step. Using CV scans and XRD to rule out changes in roughness and faceting, they interpret these results as lower temperatures effectively stabilizing Cu^+ species (by slowing the reduction kinetics of Cu^+ to Cu^0) during the cathodic pulse which enhances ethanol selectivity.

Whether the Cu electrode oxidizes during the p-eCO_2R at faster (i.e., sub-second) pulses was until recently unknown. An *in situ* XAS study by Kimura et al., found that with 50 ms pulses on polycrystalline copper, the oxidation limit can be momentarily surpassed. Even though the electrode exists above the oxidation potential where Cu_2O can thermodynamically form, oxidation is kinetically limited such that only Cu^0 exists throughout the 100 ms period ($E_a = 0.6$ V, $E_c = -1.0$ V versus RHE).[46] In addition to avoiding copper oxidation by using millisecond pulses, copper oxidation can also be avoided during longer pulses by choosing a less anodic upper potential. In experiments with longer pulse durations (5–60 s) where the anodic pulse potential is far below the equilibrium oxidation limit ($E_a = -0.8$ V versus RHE), enhanced selectivity toward CO_2R is still observed even though no oxides form.[56] Taken together, these results imply that while Cu^+ sites play a role in longer

pulse programs with sufficiently anodic upper potentials, it does not explain the p-eCO_2R behavior at shorter pulses or when the upper potential is below the oxidation potential.

Restructuring (faceting, defects) and roughening of catalyst surface

In addition to the question of the catalyst oxidation state, dynamic changes that can cause the electrode to restructure are also possible during p-eCO_2R. The question is again how fast the electrode structure may change in response to the applied potential and changing surface adsorbates. Our discussion of the electrode structure below focuses on both microscopic roughening as well as specific crystallographic faceting (and reconstruction). A voltammetric analysis carried out on a single crystal Cu(111) surface by scanning between 0 and −0.6, −0.8, and −1.2 V versus SHE clearly showed that the surface state of the catalyst can be modulated by tuning the applied potential limits.[139] A recent *in situ* electrochemical atomic force microscopy study by Simon et al. tracked nanoscale morphological changes of the Cu(100) surface under relevant cathodic potentials, observing the surface changing from granular (OCV) into smooth curved mound-pit features (−0.5 V versus RHE) or structures with rectangular terraces (−1V versus RHE).[140] Based on the results by Simon et al., morphological restructuring is clearly significant when the pulse time is greater than 1 s.

Anodic treatments can cause surface roughening.[31,48,94,96] In CO reduction experiments, Wang et al. correlated an increase in copper catalyst roughness factor to an increase in the production of C_{2+} oxygenates.[132] They demonstrated selectivity improvements were due to the high roughness factor electrodes suppressing the intrinsic activity for HER, rather than promoting CO reduction. In CO_2 reduction experiments, roughening is suggested to increase local current density (because of an increase in ECSA), which consequentially increases the local pH, thereby favoring C_2 formation.[141] However, in the work by Jiang et al., the observed enhancements during potentiostatic reduction after potential cycling their polycrystalline Cu foil could not be attributed to an increase in interfacial pH alone.[94] Instead, the intrinsic C_{2+} activity of the catalyst was changing, pointing to possible differences in faceting in addition to increased roughness. On the contrary, recent pulsing studies using short pulses ($\leq$ 1 s[46,49,52]) or less anodic upper potentials (−0.8 V versus RHE)[56] have found no noticeable change in ECSA (a roughness indicator). This suggests that changes in roughness depend on the condition of cycling and that under milder pulse conditions, roughness cannot explain the selectivity differences observed.

The restructuring mechanism of polycrystalline copper during potentiostatic eCO_2R was proposed by Kim et al., suggesting first the transformation to Cu(111), which takes 30–60 min, followed by a subsequent conversion to Cu.(100)[142–144] This process is independent of pH or electrolyte composition and is driven by the cathodic potential.[143] Work by Lee et al. also observed polycrystalline copper transforming to Cu(100), and they noted that this transformation became more pronounced with increasingly negative potential, suggesting that CO_{ads} is a key factor in promoting this reconstruction.[54] Interestingly, single crystal Cu(111) and Cu(100) catalysts do not undergo this reconstruction under relevant reduction potentials and the reason for non-reconstruction is not understood.[144] Cu(111) and Cu(100) are suggested to favor methane and ethylene, respectively,[26,145] and a recent study combining cyclic voltammetry and laser-induced temperature jump methods found that Cu(111) and Cu(100) exhibit different pzc values as well as different shifts in OH_{ads} voltammetric features.[146] Because faceting influences product selectivity and charge distribution at the interface, it is an important mechanism to consider when evaluating pulse

Please cite this article in press as: Casebolt et al., Pulse check: Potential opportunities in pulsed electrochemical CO_2 reduction, Joule (2021), https://doi.org/10.1016/j.joule.2021.05.014

methods. However, multi-hour pulsing experiments on polycrystalline copper and deoxidized high phosphorous copper did not show a shift in product selectivity that is consistent with the proposed transformation mechanism, i.e., from methane (Cu(111)) to ethylene (Cu(100)).[32,45] Thus, the simple (111)-to-(100) reconstruction mechanism cannot yet explain the observed selectivity trends in p-eCO_2R.

Potential-dependent changes in surface faceting are an important consideration as the formation of ethylene is favored on Cu(100) and methane on Cu(111) in both aqueous H-cell and gas-fed flow cells.[147,148] A recent study using ICP-MS to track the copper dissolution as a function of potential and pH during reductive/oxidative CV scans found that copper dissolution led to crystal facet modifications, and that dissolution can be avoided by staying within pH 9–10 and not exceeding the Cu^0/Cu^+ potential.[116] Arán-Ais et al. observed that pulsing creates (100) cubic islands, and that these islands are still observed after an hour of constant-potential reduction. Only when E_a is > 0.8 V versus RHE do the well-ordered domains deteriorate.[52] If changes in surface faceting were the dominant factor governing selectivity differences in p-eCO_2R, then electrodes with identical facets should exhibit the same selectivity whether or not a pulsed potential is applied. However, the experiments described by Arán-Ais et al. showed that testing a single crystal Cu(100) electrode led to 32% ethanol selectivity under pulsed conditions (E_c = −1 V, E_a = 0.8 V versus RHE, t_a= t_c = 1 s) and only 8% ethanol selectivity under potentiostatic (−1 V versus RHE) conditions; these results thus indicate that faceting is not a dominant factor for ethanol selectivity under pulsed conditions.[52]

Aside from crystallographic faceting, the grain size and grain boundary density on the electrode surface play an important role in electrocatalytic processes. It has been suggested that instead of crystal faceting, it is the crystal fragmentation caused by reduction/oxidation cycles that creates grain boundaries and an increased number of steps/edges that changes product selectivity.[120,122,149] The resulting complex grain boundary network facilitates the CO binding and increases the chances for the adjacent CO_{ads} intermediates to couple while simultaneously suppressing HER.[122] The extent of the fragmentation depends on the negative potential applied and the time spent at that potential.[122] A long-term study by Engelbrecht et al., observed differences in surface morphology after pulsing and found that grain reorganization becomes more significant as the anodic potential becomes more positive.[32] A recent study by Jeon et al. testing the application of highly oxidative pulse potentials (0.6 to 1.2 V versus RHE) on a Cu NC catalyst found that product selectivity during p-eCO_2R when $E_a \leq$ 0.9 V versus RHE was maintained even after switching to potentiostatic conditions.[96] Therefore, they suggested that pulsing resulted in irreversible changes in the catalyst morphology, and that the enhanced C_2 selectivity can be attributed to the creation of a defective surface with large grain boundaries.

Defects can be quantified using CV scans to monitor changes in defect charge.[52,150] Arán-Ais et al. applied this approach and found that defects created during pulsing do not disappear during constant-potential reduction.[52] Additionally, they observed no change in ECSA between electropolished and pulsed electrodes. Testing their Cu(100) electrode, the defect density was confirmed to be the same after pulsed (E_c = −1 V, E_a = 0.6 V versus RHE, t_c = t_a = 1 s) and constant (−1 V versus RHE) reduction. Despite no difference in defect density, they observed significant changes in the HER and ethanol selectivity. In a similar experiment tracking changes in product selectivity on a predominately (100)-textured Cu foil during pulsing over a 6 hour experiment by Tang et al., they observed increased C_2 product formation during p-eCO_2R despite no changes in roughness or faceting.[97] Rather they

Please cite this article in press as: Casebolt et al., Pulse check: Potential opportunities in pulsed electrochemical CO_2 reduction, Joule (2021), https://doi.org/10.1016/j.joule.2021.05.014

hypothesized that the continuous oxidation and reduction of the electrode under pulsed conditions created an active surface promoting CO_{ads} and enhancing C–C coupling. This hypothesis is supported by their calculations of a lower activation energy (using Arrhenius temperature dependence studies) for ethylene formation under pulsed conditions than under static conditions.

In summary, the studies described in this section illustrate that the electrode composition and structure can change during the applied pulse depending on the pulse duration and applied vertex potential. While more positive anodic potentials lead to more significant restructuring, these transformations may be kinetically avoided with short (millisecond) pulses. Moreover, further studies are required to delineate the interplay between and relative contributions of dynamic changes in adsorbate coverage and catalyst structure and composition.

Mechanism summary and emerging guidelines for future advances in peCO_2R

The mechanistic basis for product selectivity in p-eCO_2R involves a complex and dynamic interplay between several processes on both sides of the solid/electrolyte interface. Whereas this review and analysis cannot point toward a singular mechanism, we provide a general scheme for using pulsing as a "knob" to tune selectivity toward a given product.

For example, based on the information above, we outline a general scheme for C_{2+} product formation. Taking everything we have learned about pulse duration, pulse potential, mass transfer, copper oxidation, surface adsorption/desorption, and surface reconstruction, we can point to specific reaction conditions that enhance C_{2+} product formation during p-eCO_2R. For one, we would need to optimize the pulse duration so that it is long enough to enter into Regime II to avoid non-faradic current domination, which leads to increased hydrogen evolution,[48] but not too long so that we can take advantage of the transient high pH and high CO_2 concentration following a potential step.[95] We would also want to pulse on a copper catalyst with (100) facets to an anodic potential that is positive enough to regenerate Cu^+ (noting that we can affect whether ethylene or ethanol is formed by varying temperature),[52,97] but not so anodic that we lose significant amounts of the catalyst to corrosion[32] or form OH-poor environments that favor methane over C_2 products.[96] And from preliminary p-eCO_2R experiments in different electrolytes, we would want to pulse in electrolytes that have a small cation hydration radius such as Cs^+,[56] as well as in an electrolyte environment with a low availability of proton donors and increased presence of hydroxides.[45] In this way, we can begin to take advantage of all of the different mechanisms and insights outlined above to optimize for a given C_{2+} product. More generally, there are several emerging trends that are summarized below.

As one of the key experimental parameters, temporal adjustment of the pulse profile can provide control over distinct kinetic processes. Very short pulse times (milliseconds) provide control over the capacitive charging and electro-adsorption/desorption. This dynamic interfacial environment contributes significantly to the p-eCO_2R. The anodic pulse, for example, could desorb hydrogen species and adsorb hydroxides, effectively varying the ratio of adsorbed CO to H on the electrode surface to impact the reaction selectivity. At longer pulse times, on the order of seconds, surface roughening and morphological changes emerge, as well as the possible formation of persistent oxides on the surface. Additionally, CO_2 can be replenished at the surface during the "off" period. As the anodic treatment is extended to periods of

Please cite this article in press as: Casebolt et al., Pulse check: Potential opportunities in pulsed electrochemical CO_2 reduction, Joule (2021), https://doi.org/10.1016/j.joule.2021.05.014

every few hours, the benefit includes restoring the electrode to its original catalytic activity by disposing the surface of contaminations.

The applied potential is the second key experimental parameter in p-eCO_2R. The upper pulse potential determines whether or not the catalyst oxidizes. This knob provides access to the Cu^+ formation that can potentially be used to control selectivity. For upper pulse potentials below the Cu^+ formation, the selectivity impact is due to changes in the species in the EDL. For upper pulse potentials above the copper oxide formation, surface restructuring and changes in surface morphology can occur over repetitive potential cycling. However, these transformations can be kinetically avoided through judicious choice of a fast (i.e., millisecond) pulse profile. One thus cannot treat thermodynamic and kinetic aspects as distinct parameters at the pulsed solid/electrolyte interface. While this highlights the numerous outstanding questions and challenges that remain to be resolved to bring the prospect of pulse-controlled product selectivity to full fruition, in our opinion, it also provides an opportunity to fine-tune the interfacial conditions to enable selective formation of high-value products.

OUTSTANDING QUESTIONS AND FUTURE OF PULSING

Pulsing is a versatile and powerful tool in e-CO_2R, even though the underlying dynamic physicochemical processes at the solid/electrolyte interfaces are not yet fully understood. Recent years have borne witness to rapid advances in our initial understanding and various hypothesized mechanisms and future integration of *in situ* time-resolved studies hold significant potential to answer outstanding mechanistic questions. The revival of pulsed electrochemistry can leverage concurrent advances in catalyst and electrolyte system design to improve our fundamental understanding. Moreover, p-eCO_2R provides a promising technology platform for scalable deployment by virtue of its robust performance and facile adaptation to existing electrolyzer systems.

While traditional methods of product detection (GC, NMR, and LCMS) are useful to observe system performance, they lack the ability to give instantaneous information about the direct result of different pulse profiles. Techniques like DEMS[40,56] and OLEMS[35,47] are useful for characterizing the product profile within seconds, which can provide insight into reaction kinetics and eCO_2R intermediates, as well as enabling faster exploration of the pulse parameter space. Many *ex situ* surface characterization techniques have also been employed to study the catalyst surface before and after pulsing including XPS, XRD, AFM, TEM, and SEM[30,32,41,42,48,49,51,96,97]; however, as we previously mentioned, these *ex situ* methods do not necessarily represent the true surface conditions during reaction. Advances in *operando* characterization tools have and will continue to play a critical enabling role in exploring the scientific questions discussed above.[151,152] *In situ*/*operando* techniques are paramount to understanding the catalyst surface at each point in time under relevant reaction conditions.[153] As we look back on the pulsing studies included here, just recently have *operando* techniques been employed to characterize the interface (to observe catalyst chemical state and surface-adsorbed species) during reaction including *in situ*/*operando* XAS,[46,53,54,96] *quasi in situ* XPS,[52] *in situ*/*operando* Raman spectroscopy,[50,96] and *in situ* EQCM.[41] These characterization methods require highly specialized cell configurations, which makes the use of them nontrivial. As we have explained in previous sections, the CO_{ads} intermediate is suggested to be a key piece of the pulsing mechanism based on hypotheses and simplified theoretical calculations and studying the CO_{ads} species using an *operando* technique like *in situ* SEIRAS would provide valuable insight for understanding the role of

https://doi.org/10.1016/j.joule.2021.05.014

adsorbed CO and its dynamics during p-eCO_2R. There is a large need for using time-resolved operando studies to provide direct "real-time" insight into the dynamic processes taking place during pulsing.

We also motivate future theoretical works to model trends under pulsed potential conditions. While conventional tools focus on species thermodynamics, tools that include kinetic information will become increasingly important to understand the pulse mechanism in order to identify the "first-responders" to changes in potential. Further, it would be useful to have microkinetic models looking at how the energy landscape changes with the rapidly changing conditions used in p-eCO_2R.

Comprehensive and detailed documentation of all experimental details is critical for the community to reach consensus and build understanding, as well as for enabling emerging approaches with machine learning analysis of experimental systems. As we advance our knowledge of the pulsing mechanism, it has become clear that certain parameters, such as system response time, which may have been overlooked in the past, are becoming increasingly important when optimizing the pulse duration.

Another challenge is the definition of success: what is the optimal way to represent selectivity, activity, and energy efficiency? Conventionally, one would analyze the current response to determine the number of electrons input into the system, and then quantify the products to determine the number of electrons directed toward each product to determine the faradic efficiency. In this way, it is possible that the total faradic efficiency does not sum to 100% if some of the products are unaccounted for (for example, if one only quantified gaseous products) or if there was a leak in the system and products were lost before they could be measured. However, in pulse studies, it is also common for product selectivity to be reported as a normalized efficiency where instead of analyzing the charge input into the system using the measured current, one would assume that all of the products are completely accounted for, and so the total number of electrons put into the system is the number of electrons needed to make all of the products detected. In this way, the calculated product efficiencies will always sum to 100%. While the faradic efficiency is a truer selectivity calculation than a normalized efficiency because it confirms that all products are being detected, it is not trivial to extract the faradic current from short pulse profiles with large charging current contributions. The total current profile is the sum of the non-faradic current, faradic currents from CO_2R and HER, and currents from copper oxidation and reduction, all of which depend on the applied potential. Since the underlying faradic current is not likely to be constant over time, it is difficult to accurately quantify. In terms of activity, current density is an important metric because it enables a comparison between different catalysts.[154] However, this activity data can only be understood if the ECSA of the electrode is reported so that it can be determined whether the improved activity is from higher turnover or rather just from an increased number of active sites/interfacial areas.[5,154] Additionally, activity at high overpotentials is strongly influenced by concentration polarization meaning it is not an indicator of its true intrinsic activity under bulk conditions.[155] Therefore, it has been strongly recommended that intrinsic activity and selectivity conclusions be drawn from experiments carried out under conditions where the system is not mass transport limited.[5] With this in mind, it is paramount moving forward that experimental conditions are fully documented so that data can be interpreted as accurately as possible.

Beyond fundamental understandings, p-eCO_2R is a simple way to increase the experimental degrees of freedom. This additional control creates opportunities to modulate selectivity and improve catalyst lifetime in the eCO_2R. In our opinion,

there are plenty of opportunities to further explore and optimize the pulsing method. Some of these opportunities include pulsing on different metals. Initial tests on Ag, Pd, and Pb indicate that pulsing could be applied to catalysts beyond Cu, as well as on bimetallic catalyst materials. Through pulsing on different crystal facets, we can understand the morphological effects of pulsing, and through pulsing in different chemical environments, we can better understand how pulsing affects local adsorbates. There is also room for modeling and machine learning, for example, to run through a series of different pulse profiles to determine the optimum performance conditions. Finally, there is also a widely unexplored space for applying pulsing to GDE-based flow cell systems to gain additional performance by taking advantage of the faster reactant diffusion. To our knowledge, there are only three published studies evaluating pulsed electrolysis on GDEs under high current density conditions.[34,54,96] Whether the current knowledge and pulsing trends in aqueous environments can transfer directly to GDE configurations has just begun to be explored and is relatively unknown, and this is because quite a few things are different in these high-surface area high-current density devices: (1) the electrolyte flows through the cell which could possibly flush away dissolved copper ions before they are precipitated onto the surface as has been observed under some pulse conditions,[41] (2) there is now a three-phase heterogeneous reaction interface with high currents creating a very different reaction environment than when planar electrodes are used (specifically changing pH conditions, which can introduce new complexities at the surface such as CO_2 depletion, salt formation,[34] OH-poor environments,[96] etc.),[156] and (3) the larger electrode areas and higher ohmic losses can drastically change the system response time to an applied potential. We believe that addressing these challenges can increase eCO_2R's commercial viability in addition to advancing our understanding of the interplay of kinetics and transport in electrochemical systems to contribute to our understanding of electrochemical devices in general.

CONCLUSIONS

In conclusion, we provide a summary of recent advances in p-eCO_2R with a focus on the complex interplay of dynamic processes at the solid/electrolyte interface. Our review/perspective highlights the current knowledge gaps, inconsistencies, opportunities, and inspirations for future studies. We believe that addressing some of the highlighted questions can bring the broad potential of this promising approach to full fruition. We analyzed a wide variety of examples to underscore p-eCO_2R as a useful, versatile, and robust method to modify the performance of eCO_2R since it creates microenvironments that are unachievable under potentiostatic conditions. Because of the varying timescales of the dynamic processes (diffusion, adsorption/desorption, reaction) happening at the electrode interface, modulating the potential at regular intervals will have significant disruptive effects, thereby influencing the reaction environment and reaction kinetics.

The interest in p-eCO_2R is driven by its ability to improve reaction selectivity. However, as we have discussed, the pulsing mechanism is quite complex as there are multiple processes occurring at the same time: (1) changing local concentrations of reactants, products, intermediates, and spectators in the EDL, (2) restructuring of facets including oxide formation, and (3) dynamic changes in interfacial chemistry, in particular, the surface adsorbates. The extent to which these processes dominate is based on the specific applied pulse program—an opportunity for future works to identify. As CO_2 utilization becomes more critical to address the rising CO_2 levels, significant efforts will need to be put in place to continue pushing forward our

knowledge of pulse methods so that we can apply them optimally to achieve high-efficiency CO_2 valorization systems.

SUPPLEMENTAL INFORMATION

Supplemental information can be found online at https://doi.org/10.1016/j.joule.2021.05.014.

ACKNOWLEDGMENTS

Q8 This work was supported in part by the National Science Foundation (NSF; CBET1805400). R.C. was supported by the CeSI-Corning Graduate Fellowship and Cornell University Robert F. Smith School of Chemical and Biomolecular Engineering. K.L. acknowledges support from the Cornell Engineering Learning Initiative. The authors would like to thank Prof. H. Abruña for helpful discussions and review.

REFERENCES

1. Guth, U., Vonau, W., and Zosel, J. (2009). Recent developments in electrochemical sensor application and technology—a review. Meas. Sci. Technol. *20*, 042002. https://doi.org/10.1088/0957-0233/20/4/042002.

2. Petro, R., and Schlesinger, M. (2013). Applications of Electrochemistry in Medicine. In Modern Aspects of Electrochemistry, R.E. White and C.G. Vayenas, eds. (Springer), pp. 1–33.

3. Pletcher, D., and Walsh, F.C. (2012). Industrial Electrochemistry (Springer Science & Business Media).

4. Bushuyev, O.S., De Luna, P., Dinh, C.T., Tao, L., Saur, G., van de Lagemaat, J., Kelley, S.O., and Sargent, E.H. (2018). What should we make with CO_2 and how can we make it? Joule *2*, 825–832. https://doi.org/10.1016/j.joule.2017.09.003.

5. Nitopi, S., Bertheussen, E., Scott, S.B., Liu, X., Engstfeld, A.K., Horch, S., Seger, B., Stephens, I.E.L., Chan, K., Hahn, C., et al. (2019). Progress and perspectives of electrochemical CO2 reduction on copper in aqueous electrolyte. Chem. Rev. *119*, 7610–7672. https://doi.org/10.1021/acs.chemrev.8b00705.

6. Hori, Y. (2008). Electrochemical CO_2 reduction on metal electrodes. In Modern Aspects of Electrochemistry, C.G. Vayenas, R.E. White, and M.E. Gamboa-Aldeco, eds. (Springer), pp. 89–189.

7. Verma, S., Kim, B., Jhong, H.", Ma, S., and Kenis, P.J.A. (2016). A gross-margin model for defining technoeconomic benchmarks in the electroreduction of CO2. ChemSusChem *9*, 1972–1979. https://doi.org/10.1002/cssc.201600394.

8. Kumar, B., Brian, J.P., Atla, V., Kumari, S., Bertram, K.A., White, R.T., and Spurgeon, J.M. (2016). New trends in the development of heterogeneous catalysts for electrochemical CO2 reduction. Catal. Today *270*, 19–30. https://doi.org/10.1016/j.cattod.2016.02.006.

9. Liu, A., Gao, M., Ren, X., Meng, F., Yang, Y., Gao, L., Yang, Q., and Ma, T. (2020). Current progress in electrocatalytic carbon dioxide reduction to fuels on heterogeneous catalysts. J. Mater. Chem. A *8*, 3541–3562. https://doi.org/10.1039/C9TA11966C.

10. Long, C., Li, X., Guo, J., Shi, Y., Liu, S., and Tang, Z. (2019). Electrochemical reduction of CO2 over heterogeneous catalysts in aqueous solution: recent progress and perspectives. Small Methods *3*, 1800369. https://doi.org/10.1002/smtd.201800369.

11. Qiao, J., Liu, Y., Hong, F., and Zhang, J. (2014). A review of catalysts for the electroreduction of carbon dioxide to produce low-carbon fuels. Chem. Soc. Rev. *43*, 631–675. https://doi.org/10.1039/C3CS60323G.

12. Fan, L., Xia, C., Yang, F., Wang, J., Wang, H., and Lu, Y. (2020). Strategies in catalysts and electrolyzer design for electrochemical CO2 reduction toward C2+ products. Sci. Adv. *6*, eaay3111. https://doi.org/10.1126/sciadv.aay3111.

13. Liang, S., Altaf, N., Huang, L., Gao, Y., and Wang, Q. (2020). Electrolytic cell design for electrochemical CO2 reduction. J. CO2 Util. *35*, 90–105. https://doi.org/10.1016/j.jcou.2019.09.007.

14. Vennekoetter, J.-B., Sengpiel, R., and Wessling, M. (2019). Beyond the catalyst: how electrode and reactor design determine the product spectrum during electrochemical CO2 reduction. Chem. Eng. J. *364*, 89–101. https://doi.org/10.1016/j.cej.2019.01.045.

15. Tufa, R.A., Chanda, D., Ma, M., Aili, D., Demissie, T.B., Vaes, J., Li, Q., Liu, S., and Pant, D. (2020). Towards highly efficient electrochemical CO2 reduction: cell designs, membranes and electrocatalysts. Appl. Energy *277*, 115557. https://doi.org/10.1016/j.apenergy.2020.115557.

16. Higgins, D., Hahn, C., Xiang, C., Jaramillo, T.F., and Weber, A.Z. (2019). Gas-diffusion electrodes for carbon dioxide reduction: a new paradigm. ACS Energy Lett *4*, 317–324. https://doi.org/10.1021/acsenergylett.8b02035.

17. Moura de Salles Pupo, M., and Kortlever, R. (2019). Electrolyte effects on the electrochemical reduction of CO2. ChemPhysChem *20*, 2926–2935. https://doi.org/10.1002/cphc.201900680.

18. Lu, Q., and Jiao, F. (2016). Electrochemical CO2 reduction: electrocatalyst, reaction mechanism, and process engineering. Nano Energy *29*, 439–456. https://doi.org/10.1016/j.nanoen.2016.04.009.

19. Gao, D., Arán-Ais, R.M., Jeon, H.S., and Roldan Cuenya, B.R. (2019). Rational catalyst and electrolyte design for CO2 electroreduction towards multicarbon products. Nat. Catal. *2*, 198–210. https://doi.org/10.1038/s41929-019-0235-5.

20. Greenblatt, J.B., Miller, D.J., Ager, J.W., Houle, F.A., and Sharp, I.D. (2018). The technical and energetic challenges of separating (photo)electrochemical carbon dioxide reduction products. Joule *2*, 381–420. https://doi.org/10.1016/j.joule.2018.01.014.

21. National Research Council (2005). Sustainability in the Chemical Industry: Grand Challenges and Research Needs (National Academies Press).

22. Sholl, D.S., and Lively, R.P. (2016). Seven chemical separations to change the world. Nature *532*, 435–437.

23. Kuhl, K.P., Hatsukade, T., Cave, E.R., Abram, D.N., Kibsgaard, J., and Jaramillo, T.F. (2014). Electrocatalytic conversion of carbon dioxide to methane and methanol on transition metal surfaces. J. Am. Chem. Soc. *136*, 14107–14113. https://doi.org/10.1021/ja505791r.

24. Bagger, A., Ju, W., Varela, A.S., Strasser, P., and Rossmeisl, J. (2017). Electrochemical CO2 reduction: a classification problem. ChemPhysChem *18*, 3266–3273. https://doi.org/10.1002/cphc.201700736.

25. Wuttig, A., Liu, C., Peng, Q., Yaguchi, M., Hendon, C.H., Motobayashi, K., Ye, S., Osawa, M., and Surendranath, Y. (2016). Tracking a common surface-bound intermediate during CO2-to-fuels catalysis. ACS Cent. Sci. *2*, 522–528. https://doi.org/10.1021/acscentsci.6b00155.

26. Clark, E.L., and Bell, A.T. (2021). Heterogeneous electrochemical CO2 reduction. In Carbon Dioxide Electrochemistry: Homogeneous and Heterogeneous Catalysis, C.C. Marc Robert and K. Daasbjerg, eds. (The Royal Society of Chemistry)), pp. 98–150.

27. Kuhl, K.P., Cave, E.R., Abram, D.N., and Jaramillo, T.F. (2012). New insights into the electrochemical reduction of carbon dioxide on metallic copper surfaces. Energy Environ. Sci. *5*, 7050–7059. https://doi.org/10.1039/C2EE21234J.

28. DeWulf, D.W., Jin, T., and Bard, A.J. (1989). Electrochemical and surface studies of carbon dioxide reduction to methane and ethylene at copper electrodes in aqueous solutions. J. Electrochem. Soc. *136*, 1686–1691. https://doi.org/10.1149/1.2096993.

29. Hori, Y., Konishi, H., Futamura, T., Murata, A., Koga, O., Sakurai, H., and Oguma, K. (2005). Deactivation of copper electrode" in electrochemical reduction of CO2. Electrochim. Acta *50*, 5354–5369. https://doi.org/10.1016/j.electacta.2005.03.015.

30. Shiratsuchi, R., Aikoh, Y., and Nogami, G. (1993). Pulsed electroreduction of CO2 on Copper electrodes. J. Electrochem. Soc. *140*, 3479–3482. https://doi.org/10.1149/1.2221113.

31. Jermann, B., and Augustynski, J. (1994). Long-term activation of the copper cathode in the course of CO2 reduction. Electrochim. Acta *39*, 1891–1896. https://doi.org/10.1016/0013-4686(94)85181-6.

32. Engelbrecht, A., Uhlig, C., Stark, O., Hämmerle, M., Schmid, G., Magori, E., Wiesner-Fleischer, K., Fleischer, M., and Moos, R. (2018). On the electrochemical CO2 reduction at copper sheet electrodes with enhanced long-term stability by pulsed electrolysis. J. Electrochem. Soc. *165*, J3059–J3068. https://doi.org/10.1149/2.0091815jes.

33. Lee, C.W., Cho, N.H., Nam, K.T., Hwang, Y.J., and Min, B.K. (2019). Cyclic two-step electrolysis for stable electrochemical conversion of carbon dioxide to formate. Nat. Commun. *10*, 3919. https://doi.org/10.1038/s41467-019-11903-5.

34. Xu, Y., Edwards, J.P., Liu, S., Miao, R.K., Huang, J.E., Gabardo, C.M., O'Brien, C.P., Li, J., Sargent, E.H., and Sinton, D. (2021). Self-cleaning CO2 reduction systems: unsteady electrochemical forcing enables stability. ACS Energy Lett *6*, 809–815. https://doi.org/10.1021/acsenergylett.0c02401.

35. Wasmus, S., Cattaneo, E., and Vielstich, W. (1990). Reduction of carbon dioxide to methane and ethene—an on-line MS study with rotating electrodes. Electrochim. Acta *35*, 771–775. https://doi.org/10.1016/0013-4686(90)90014-O.

36. Nogami, G., Itagaki, H., and Shiratsuchi, R. (1994). Pulsed electroreduction of CO2 on Copper electrodes-II. J. Electrochem. Soc. *141*, 1138–1142. https://doi.org/10.1149/1.2054886.

37. Ishimaru, S., Shiratsuchi, R., and Nogami, G. (2000). Pulsed electroreduction of CO2 on Cu-Ag alloy electrodes. J. Electrochem. Soc. *147*, 1864. https://doi.org/10.1149/1.1393448.

38. Shiratsuchi, R., and Nogami, G. (1996). Pulsed electroreduction of CO2 on Silver electrodes. J. Electrochem. Soc. *143*, 582–586. https://doi.org/10.1149/1.1836484.

39. Kedzierzawski, P., and Augustynski, J. (1994). Poisoning and activation of the gold cathode during electroreduction of CO2. J. Electrochem. Soc. *141*, L58–L60. https://doi.org/10.1149/1.2054936.

40. Friebe, P., Bogdanoff, P., Alonso-Vante, N., and Tributsch, H. (1997). A real-time mass spectroscopy study of the (electro)chemical factors affecting CO2reduction at copper. J. Catal. *168*, 374–385. https://doi.org/10.1006/jcat.1997.1606.

41. Lee, J., and Tak, Y. (2001). Electrocatalytic activity of Cu electrode in electroreduction of CO2. Electrochim. Acta *46*, 3015–3022. https://doi.org/10.1016/S0013-4686(01)00527-8.

42. Yano, J., and Yamasaki, S. (2008). Pulse-mode electrochemical reduction of carbon dioxide using copper and copper oxide electrodes for selective ethylene formation. J. Appl. Electrochem. *38*, 1721–1726. https://doi.org/10.1007/s10800-008-9622-3.

43. Gupta, N., Gattrell, M., and MacDougall, B. (2006). Calculation for the cathode surface concentrations in the electrochemical reduction of CO2 in KHCO3 solutions. J. Appl. Electrochem. *36*, 161–172. https://doi.org/10.1007/s10800-005-9058-y.

44. Kimura, K.W., Fritz, K.E., Kim, J., Suntivich, J., Abruña, H.D., and Hanrath, T. (2018). Controlled selectivity of CO2 reduction on copper by pulsing the electrochemical potential. ChemSusChem *11*, 1781–1786. https://doi.org/10.1002/cssc.201800318.

45. Casebolt, R., Kimura, K.W., Levine, K., Cimada Dasilva, J.A., Kim, J., Dunbar, T.A., Suntivich, J., and Hanrath, T. (2021). Effect of electrolyte composition and concentration on pulsed potential electrochemical CO2 reduction. ChemElectroChem *8*, 681–688. https://doi.org/10.1002/celc.202001445.

46. Kimura, K.W., Casebolt, R., Cimada Dasilva, J., Kauffman, E., Kim, J., Dunbar, T.A., Pollock, C.J., Suntivich, J., and Hanrath, T. (2020). Selective electrochemical CO2 reduction during pulsed potential stems from dynamic interface. ACS Catal *10*, 8632–8639. https://doi.org/10.1021/acscatal.0c02630.

47. Le Duff, C.S., Lawrence, M.J., and Rodríguez, P. (2017). Role of the adsorbed oxygen species in the selective electrochemical reduction of CO2 to alcohols and carbonyls on copper electrodes. Angew. Chem. Int. Ed. Engl. *56*, 12919–12924. https://doi.org/10.1002/anie.201706463.

48. Kumar, B., Brian, J.P., Atla, V., Kumari, S., Bertram, K.A., White, R.T., and Spurgeon, J.M. (2016). Controlling the product syngas H2:CO Ratio through pulsed-bias electrochemical reduction of CO2on copper. ACS Catal *6*, 4739–4745. https://doi.org/10.1021/acscatal.6b00857.

49. Strain, J.M., Gulati, S., Pishgar, S., and Spurgeon, J.M. (2020). Pulsed electrochemical carbon monoxide reduction on oxide-derived copper catalyst. ChemSusChem *13*, 3028–3033. https://doi.org/10.1002/cssc.202000464.

50. Blom, M.J.W., Smulders, V., van Swaaij, W.P.M., Kersten, S.R.A., and Mul, G. (2020). Pulsed electrochemical synthesis of formate using Pb electrodes. Appl. Catal. B *268*, 118420. https://doi.org/10.1016/j.apcatb.2019.118420.

51. Lim, C.F.C., Harrington, D.A., and Marshall, A.T. (2016). Altering the selectivity of galvanostatic CO2 reduction on Cu cathodes by periodic cyclic voltammetry and potentiostatic steps. Electrochim. Acta *222*, 133–140. https://doi.org/10.1016/j.electacta.2016.10.185.

52. Arán-Ais, R.M., Scholten, F., Kunze, S., Rizo, R., and Roldan Cuenya, B.R. (2020). The role of in situ generated morphological motifs and Cu(I) species in C2+ product selectivity during CO2 pulsed electroreduction. Nat. Energy *5*, 317–325. https://doi.org/10.1038/s41560-020-0594-9.

53. Lin, S.C., Chang, C.C., Chiu, S.Y., Pai, H.T., Liao, T.Y., Hsu, C.S., Chiang, W.H., Tsai, M.K., and Chen, H.M. (2020). Operando time-resolved X-ray absorption spectroscopy reveals the chemical nature enabling highly selective CO2 reduction. Nat. Commun. *11*, 3525. https://doi.org/10.1038/s41467-020-17231-3.

54. Lee, S.H., Sullivan, I., Larson, D.M., Liu, G., Toma, F.M., Xiang, C., and Drisdell, W.S. (2020). Correlating oxidation state and surface area to activity from operando studies of Copper CO electroreduction catalysts in a gas-fed device. ACS Catal *10*, 8000–8011. https://doi.org/10.1021/acscatal.0c01670.

55. Oguma, T., and Azumi, K. (2020). Improvement of electrochemical reduction of CO2 using the potential-pulse polarization method. Electrochemistry *88*, 451–456. https://doi.org/10.5796/electrochemistry.20-00037.

56. Kim, C., Weng, L.-C., and Bell, A.T. (2020). The impact of pulsed electrochemical reduction of CO2 on the formation of C2+ products over Cu. ACS Catal *10*, 12403–12413. https://doi.org/10.1021/acscatal.0c02915.

57. Jännsch, Y., Leung, J.J., Hämmerle, M., Magori, E., Wiesner-Fleischer, K., Simon, E., Fleischer, M., and Moos, R. (2020). Pulsed potential electrochemical CO2 reduction for enhanced stability and catalyst reactivation of copper electrodes. Electrochem. Commun. *121*, 106861. https://doi.org/10.1016/j.elecom.2020.106861.

58. Popović, S., Smiljanić, M., Jovanovič, P., Vavra, J., Buonsanti, R., and Hodnik, N. (2020). Stability and degradation mechanisms of copper-based catalysts for electrochemical CO2 reduction. Angew. Chem. Int. Ed. Engl. *59*, 14736–14746. https://doi.org/10.1002/anie.202000617.

59. Karaiskakis, A.N., Goltu, S.S., and Biddinger, E.J. (2019). Effect of electrode geometry on selectivity and activity in CO2 electroreduction. Ind. Eng. Chem. Res. *58*, 22506–22515. https://doi.org/10.1021/acs.iecr.9b03762.

60. Klingan, K., Kottakkat, T., Jovanov, Z.P., Jiang, S., Pasquini, C., Scholten, F., Kubella, P., Bergmann, A., Roldan Cuenya, B.R., Roth, C., and Dau, H. (2018). Reactivity determinants in electrodeposited Cu foams for electrochemical CO2 reduction. ChemSusChem *11*, 3449–3459. https://doi.org/10.1002/cssc.201801582.

61. Lee, C.W., Yang, K.D., Nam, D.H., Jang, J.H., Cho, N.H., Im, S.W., and Nam, K.T. (2018). Defining a materials database for the design of copper binary alloy catalysts for electrochemical CO2 conversion. Adv. Mater. *30*, e1704717. https://doi.org/10.1002/adma.201704717.

62. Blanco, D.E., Lee, B., and Modestino, M.A. (2019). Optimizing organic electrosynthesis through controlled voltage dosing and artificial intelligence. Proc. Natl. Acad. Sci. USA *116*, 17683–17689. https://doi.org/10.1073/pnas.1909985116.

63. Sattler, L.E., Otten, C.J., and Hilt, G. (2020). Alternating current electrolysis for the electrocatalytic synthesis of mixed disulfide via sulfur–sulfur bond metathesis towards dynamic disulfide libraries. Chem. Eur. J. *26*, 3129–3136. https://doi.org/10.1002/chem.201904948.

64. Savett, S.C., Lee, S.M., Bradley, A.Z., Kneizys, S.P., LoBue, J.M., and Middleton, W.J. (1993). Microscale electrolytic fluorinations of 4-nitrotoluene - cell construction, computer monitor and control, and chemistry. Microchem. J. *48*, 192–199. https://doi.org/10.1006/mchj.1993.1090.

65. Lee, S.M., Roseman, J.M., Blair Zartman, C.B., Morrison, E.P., Harrison, S.J., Stankiewicz, C.A., and Middleton, W.J. (1996). Selective electrolytic fluorinations in 70% HF/30% pyridine. J. Fluor. Chem. *77*, 65–70. https://doi.org/10.1016/0022-1139(95)03379-3.

66. Lee, B., Naito, H., Nagao, M., and Hibino, T. (2012). Alternating-current electrolysis for the production of phenol from benzene. Angew. Chem. Int. Ed. Engl. *51*, 6961–6965. https://doi.org/10.1002/anie.201202159.

67. Schotten, C., Taylor, C.J., Bourne, R.A., Chamberlain, T.W., Nguyen, B.N., Kapur, N., and Willans, C.E. (2020). Alternating polarity for enhanced electrochemical synthesis. React. Chem. Eng. *6*, 147–151. https://doi.org/10.1039/D0RE00399A.

68. Rodrigo, S., Um, C., Mixdorf, J.C., Gunasekera, D., Nguyen, H.M., and Luo, L. (2020). Alternating current electrolysis for organic electrosynthesis: trifluoromethylation of (hetero)arenes. Org. Lett. *22*, 6719–6723. https://doi.org/10.1021/acs.orglett.0c01906.

69. Román, A.M., Spivey, T.D., Medlin, J.W., and Holewinski, A. (2020). Accelerating electro-oxidation turnover rates via potential-modulated stimulation of electrocatalytic activity. Ind. Eng. Chem. Res. *59*, 19999–20010. https://doi.org/10.1021/acs.iecr.0c04414.

70. Vehrenberg, J., Vepsäläinen, M., Macedo, D.S., Rubio-Martinez, M., Webster, N.A.S., and Wessling, M. (2020). Steady-state electrochemical synthesis of HKUST-1 with polarity reversalmytitlenote. Micropor. Mesopor. Mater. *303*, 110218. https://doi.org/10.1016/j.micromeso.2020.110218.

71. Xu, J., Liu, C., Hsu, P.C., Zhao, J., Wu, T., Tang, J., Liu, K., and Cui, Y. (2019). Remediation of heavy metal contaminated soil by asymmetrical alternating current electrochemistry. Nat. Commun. *10*, 2440. https://doi.org/10.1038/s41467-019-10472-x.

72. Karamati-Niaragh, E., Alavi Moghaddam, M.R.A., Emamjomeh, M.M., and Nazlabadi, E. (2019). Evaluation of direct and alternating current on nitrate removal using a continuous electrocoagulation process: economical and environmental approaches through RSM. J. Environ. Manage. *230*, 245–254. https://doi.org/10.1016/j.jenvman.2018.09.091.

73. Liu, C., Hsu, P.-C., Xie, J., Zhao, J., Wu, T., Wang, H., Liu, W., Zhang, J., Chu, S., and Cui, Y. (2017). A half-wave rectified alternating current electrochemical method for uranium extraction from seawater. Nat. Energy *2*, 17007. https://doi.org/10.1038/nenergy.2017.7.

74. Zhou, L., Liu, D., Li, S., Yin, X., Zhang, C., Li, X., Zhang, C., Zhang, W., Cao, X., Wang, J., and Wang, Z.L. (2019). Effective removing of hexavalent chromium from wasted water by triboelectric nanogenerator driven self-powered electrochemical system – Why pulsed DC is better than continuous DC? Nano Energy *64*, 103915. https://doi.org/10.1016/j.nanoen.2019.103915.

75. Raut, A.S., Parker, C.B., Klem, E.J.D., Stoner, B.R., Deshusses, M.A., and Glass, J.T. (2019). Reduction in energy for electrochemical disinfection of E. coli in urine simulant. J. Appl. Electrochem. *49*, 443–453. https://doi.org/10.1007/s10800-019-01292-4.

76. Carpanedo de Morais Nepel, T., Landers, R., Gurgel Adeodato Vieira, M., and Florêncio de Almeida Neto, A. (2020). Metallic copper removal optimization from real wastewater using pulsed electrodeposition. J. Hazard. Mater. *384*, 121416. https://doi.org/10.1016/j.jhazmat.2019.121416.

77. Stamenkovic, V.R., Strmcnik, D., Lopes, P.P., and Markovic, N.M. (2016). Energy and fuels from electrochemical interfaces. Nat. Mater. *16*, 57–69. https://doi.org/10.1038/nmat4738.

78. Bard, A.J., and Faulkner, L.R. (2001). Electrochemical Methods Fundamentals and Applications (John Wiley & Sons).

79. Wang, J. (2006). Analytical Electrochemistry (John Wiley & Sons).

80. Ringe, S., Clark, E.L., Resasco, J., Walton, A., Seger, B., Bell, A.T., and Chan, K. (2019). Understanding cation effects in electrochemical CO2 reduction. Energy Environ. Sci. *12*, 3001–3014. https://doi.org/10.1039/C9EE01341E.

81. Resasco, J., Chen, L.D., Clark, E., Tsai, C., Hahn, C., Jaramillo, T.F., Chan, K., and Bell, A.T. (2017). Promoter effects of alkali metal cations on the electrochemical reduction of carbon dioxide. J. Am. Chem. Soc. *139*, 11277–11287. https://doi.org/10.1021/jacs.7b06765.

82. Singh, M.R., Kwon, Y., Lum, Y., Ager, J.W., III, and Bell, A.T. (2016). Hydrolysis of electrolyte cations enhances the electrochemical reduction of CO2 over Ag and Cu. J. Am. Chem. Soc. *138*, 13006–13012. https://doi.org/10.1021/jacs.6b07612.

83. Varela, A.S., Kroschel, M., Reier, T., and Strasser, P. (2016). Controlling the selectivity of CO2 electroreduction on copper: the effect of the electrolyte concentration and the importance of the local pH. Catal. Today *260*, 8–13. https://doi.org/10.1016/j.cattod.2015.06.009.

84. Resasco, J., Lum, Y., Clark, E., Zeledon, J.Z., and Bell, A.T. (2018). Effects of anion identity and concentration on electrochemical reduction of CO2. ChemElectroChem *5*, 1064–1072. https://doi.org/10.1002/celc.201701316.

85. Zhao, M., Tang, H., Yang, Q., Gu, Y., Zhu, H., Yan, S., and Zou, Z. (2020). Inhibiting hydrogen evolution using a chloride adlayer for efficient electrochemical CO2 reduction on Zn electrodes. ACS Appl. Mater. Interfaces *12*, 4565–4571. https://doi.org/10.1021/acsami.9b22811.

86. Huang, Y., Ong, C.W., and Yeo, B.S. (2018). Effects of electrolyte anions on the reduction of carbon dioxide to ethylene and ethanol on copper (100) and (111) surfaces. ChemSusChem *11*, 3299–3306. https://doi.org/10.1002/cssc.201801078.

87. Bartholomew, C.H. (2001). Mechanisms of catalyst deactivation. Appl. Catal. A *212*, 17–60. https://doi.org/10.1016/S0926-860X(00)00843-7.

88. Wuttig, A., and Surendranath, Y. (2015). Impurity ion complexation enhances carbon dioxide reduction catalysis. ACS Catal *5*, 4479–4484. https://doi.org/10.1021/acscatal.5b00808.

89. Leung, K.Y., and McCrory, C.C.L. (2019). Effect and prevention of trace Ag+ contamination from Ag/AgCl reference electrodes on CO2 reduction product distributions at polycrystalline Copper electrodes. ACS Appl. Energy Mater. *2*, 8283–8293. https://doi.org/10.1021/acsaem.9b01759.

90. Jovanov, Z.P., Ferreira de Araujo, J., Li, S., and Strasser, P. (2019). Catalyst preoxidation and EDTA electrolyte additive remedy activity and selectivity declines during electrochemical CO2 reduction. J. Phys. Chem. C *123*, 2165–2174. https://doi.org/10.1021/acs.jpcc.8b08794.

91. Tiwari, A., Maagaard, T., Chorkendorff, I., and Horch, S. (2019). Effect of dissolved glassware on the structure-sensitive part of the Cu (111) voltammogram in KOH. ACS Energy Lett *4*, 1645–1649. https://doi.org/10.1021/acsenergylett.9b01064.

92. Teeter, T.E., and Van Rysselberghe, P. (1954). Reduction of carbon dioxide on mercury cathodes. J. Chem. Phys. *22*, 759–760. https://doi.org/10.1063/1.1740178.

93. Yano, J., Morita, T., Shimano, K., Nagami, Y., and Yamasaki, S. (2007). Selective ethylene formation by pulse-mode electrochemical reduction of carbon dioxide using copper and copper-oxide electrodes. J. Solid State Electrochem. *11*, 554–557. https://doi.org/10.1007/s10008-006-0181-4.

94. Jiang, K., Sandberg, R.B., Akey, A.J., Liu, X., Bell, D.C., Nørskov, J.K., Chan, K., and Wang, H. (2018). Metal ion cycling of Cu foil for selective C–C coupling in electrochemical CO2 reduction. Nat. Catal. *1*, 111–119. https://doi.org/10.1038/s41929-017-0009-x.

95. Bui, J.C., Kim, C., Weber, A.Z., and Bell, A.T. (2021). Dynamic boundary layer simulation of pulsed CO2 electrolysis on a copper catalyst.

ACS Energy Lett 6, 1181–1188. https://doi.org/10.1021/acsenergylett.1c00364.

96. Jeon, H.S., Timoshenko, J., Rettenmaier, C., Herzog, A., Yoon, A., Chee, S.W., Oener, S., Hejral, U., Haase, F.T., and Roldan Cuenya, B. (2021). Selectivity control of Cu nanocrystals in a gas-fed flow cell through CO2 pulsed electroreduction. J. Am. Chem. Soc. 143, 7578–7587. https://doi.org/10.1021/jacs.1c03443.

97. Tang, Z., Nishiwaki, E., Fritz, K.E., Hannah, T., and Suntivich, J. (2021). Cu(I) reducibility controls ethylene vs ethanol selectivity on (100)-textured copper during pulsed CO2 reduction. ACS Appl. Mater. Interfaces 13, 14050–14055. https://doi.org/10.1021/acsami.0c17668.

98. Chernyshova, I.V., Somasundaran, P., and Ponnurangam, S. (2018). On the origin of the elusive first intermediate of CO2 electroreduction. Proc. Natl. Acad. Sci. USA 115, E9261–E9270. https://doi.org/10.1073/pnas.1802256115.

99. Fan, Q., Zhang, M., Jia, M., Liu, S., Qiu, J., and Sun, Z. (2018). Electrochemical CO2 reduction to C2+ species: heterogeneous electrocatalysts, reaction pathways, and optimization strategies. Mater. Today Energy 10, 280–301. https://doi.org/10.1016/j.mtener.2018.10.003.

100. Iijima, G., Inomata, T., Yamaguchi, H., Ito, M., and Masuda, H. (2019). Role of a hydroxide layer on Cu electrodes in electrochemical CO2 reduction. ACS Catal 9, 6305–6319. https://doi.org/10.1021/acscatal.9b00896.

101. Kuai, C., Xu, Z., Xi, C., Hu, A., Yang, Z., Zhang, Y., Sun, C.-J., Li, L., Sokaras, D., Dong, C., et al. (2020). Phase segregation reversibility in mixed-metal hydroxide water oxidation catalysts. Nat. Catal. 3, 743–753. https://doi.org/10.1038/s41929-020-0496-z.

102. Dinh, C.T., Burdyny, T., Kibria, M.G., Seifitokaldani, A., Gabardo, C.M., García de Arquer, F.P.G., Kiani, A., Edwards, J.P., De Luna, P., Bushuyev, O.S., et al. (2018). CO2 electroreduction to ethylene via hydroxide-mediated copper catalysis at an abrupt interface. Science 360, 783–787. https://doi.org/10.1126/science.aas9100.

103. Chou, T.C., Chang, C.C., Yu, H.L., Yu, W.Y., Dong, C.L., Velasco-Vélez, J.J., Chuang, C.H., Chen, L.C., Lee, J.F., Chen, J.-M., et al. (2020). Controlling the oxidation state of the Cu electrode and reaction intermediates for electrochemical CO2 reduction to ethylene. J. Am. Chem. Soc. 142, 2857–2867. https://doi.org/10.1021/jacs.9b11126.

104. Gunathunge, C.M., Ovalle, V.J., Li, Y., Janik, M.J., and Waegele, M.M. (2018). Existence of an electrochemically inert CO population on Cu electrodes in alkaline pH. ACS Catal 8, 7507–7516. https://doi.org/10.1021/acscatal.8b01552.

105. Schreier, M., Yoon, Y., Jackson, M.N., and Surendranath, Y. (2018). Competition between H and CO for active sites governs copper-mediated electrosynthesis of hydrocarbon fuels. Angew. Chem. Int. Ed. Engl. 57, 10221–10225. https://doi.org/10.1002/anie.201806051.

106. Hori, Y., Koga, O., Watanabe, Y., and Matsuo, T. (1998). FTIR measurements of charge displacement adsorption of CO on poly-and single crystal (100) of Cu electrodes. Electrochim. Acta 44, 1389–1395. https://doi.org/10.1016/S0013-4686(98)00261-8.

107. Beverskog, B., and Puigdomenech, I. (1997). Revised Pourbaix diagrams for copper at 25 to 300°C. J. Electrochem. Soc. 144, 3476–3483. https://doi.org/10.1149/1.1838036.

108. Eilert, A., Cavalca, F., Roberts, F.S., Osterwalder, J., Liu, C., Favaro, M., Crumlin, E.J., Ogasawara, H., Friebel, D., Pettersson, L.G., and Nilsson, A. (2017). Subsurface oxygen in oxide-derived copper electrocatalysts for carbon dioxide reduction. J. Phys. Chem. Lett. 8, 285–290. https://doi.org/10.1021/acs.jpclett.6b02273.

109. Gao, D., Zegkinoglou, I., Divins, N.J., Scholten, F., Sinev, I., Grosse, P., and Roldan Cuenya, B. (2017). Plasma-activated copper nanocube catalysts for efficient carbon dioxide electroreduction to hydrocarbons and alcohols. ACS Nano 11, 4825–4831. https://doi.org/10.1021/acsnano.7b01257.

110. Favaro, M., Xiao, H., Cheng, T., Goddard, W.A., Yano, J., and Crumlin, E.J. (2017). Subsurface oxide plays a critical role in CO2 activation by Cu (111) surfaces to form chemisorbed CO2, the first step in reduction of CO2. Proc. Natl. Acad. Sci. USA 114, 6706–6711. https://doi.org/10.1073/pnas.1701405114.

111. Mistry, H., Varela, A.S., Bonifacio, C.S., Zegkinoglou, I., Sinev, I., Choi, Y.W., Kisslinger, K., Stach, E.A., Yang, J.C., Strasser, P., and Cuenya, B.R. (2016). Highly selective plasma-activated copper catalysts for carbon dioxide reduction to ethylene. Nat. Commun. 7, 12123. https://doi.org/10.1038/ncomms12123.

112. Gao, D., Sinev, I., Scholten, F., Arán-Ais, R.M., Divins, N.J., Kvashnina, K., Timoshenko, J., and Roldan Cuenya, B. (2019). Selective CO2 electroreduction to ethylene and multicarbon alcohols via electrolyte-driven nanostructuring. Angew. Chem. Int. Ed. Engl. 58, 17047–17053. https://doi.org/10.1002/anie.201910155.

113. Lee, S., Kim, D., and Lee, J. (2015). Electrocatalytic production of C3-C4 compounds by conversion of CO2 on a chloride-induced bi-phasic Cu2O-Cu catalyst. Angew. Chem. Int. Ed. Engl. 54, 14701–14705. https://doi.org/10.1002/anie.201505730.

114. Lee, S.Y., Jung, H., Kim, N.K., Oh, H.S., Min, B.K., and Hwang, Y.J. (2018). Mixed copper states in anodized Cu electrocatalyst for stable and selective ethylene production from CO2 reduction. J. Am. Chem. Soc. 140, 8681–8689. https://doi.org/10.1021/jacs.8b02173.

115. Cavalca, F., Ferragut, R., Aghion, S., Eilert, A., Diaz-Morales, O., Liu, C., Koh, A.L., Hansen, T.W., Pettersson, L.G.M., and Nilsson, A. (2017). Nature and distribution of stable subsurface oxygen in copper electrodes during electrochemical CO2 reduction. J. Phys. Chem. C 121, 25003–25009. https://doi.org/10.1021/acs.jpcc.7b08278.

116. Speck, F.D., and Cherevko, S. (2020). Electrochemical copper dissolution: A benchmark for stable CO2 reduction on copper electrocatalysts. Electrochem. Commun. 115. https://doi.org/10.1016/j.elecom.2020.106739.

117. Garza, A.J., Bell, A.T., and Head-Gordon, M. (2018). Is subsurface oxygen necessary for the electrochemical reduction of CO2 on copper? J. Phys. Chem. Lett. 9, 601–606. https://doi.org/10.1021/acs.jpclett.7b03180.

118. Lum, Y., and Ager, J.W. (2018). Stability of residual oxides in oxide-derived copper catalysts for electrochemical CO2 reduction investigated with 18O labeling. Angew. Chem. Int. Ed. Engl. 57, 551–554. https://doi.org/10.1002/anie.201710590.

119. Scott, S.B., Hogg, T.V., Landers, A.T., Maagaard, T., Bertheussen, E., Lin, J.C., Davis, R.C., Beeman, J.W., Higgins, D., Drisdell, W.S., et al. (2019). Absence of oxidized phases in Cu under CO reduction conditions. ACS Energy Lett 4, 803–804. https://doi.org/10.1021/acsenergylett.9b00172.

120. Zhu, P., and Wang, H. (2020). Structural evolution of oxide-/hydroxide-derived copper electrodes accounts for the enhanced C2+ product selectivity during electrochemical CO2 reduction. Science Bulletin 65, 977–979. https://doi.org/10.1016/j.scib.2020.03.030.

121. Kim, Y.-G., and Soriaga, M.P. (2014). Cathodic regeneration of a clean and ordered Cu (1 0 0)-(1× 1) surface from an air-oxidized and disordered electrode: an operando STM study. J. Electroanal. Chem. 734, 7–9. https://doi.org/10.1016/j.jelechem.2014.09.010.

122. Lei, Q., Zhu, H., Song, K., Wei, N., Liu, L., Zhang, D., Yin, J., Dong, X., Yao, K., Wang, N., et al. (2020). Investigating the origin of enhanced C2+ selectivity in oxide-/hydroxide-derived copper electrodes during CO2 electroreduction. J. Am. Chem. Soc. 142, 4213–4222. https://doi.org/10.1021/jacs.9b11790.

123. Ren, D., Fong, J., and Yeo, B.S. (2018). The effects of currents and potentials on the selectivities of copper toward carbon dioxide electroreduction. Nat. Commun. 9, 925. https://doi.org/10.1038/s41467-018-03286-w.

124. Mandal, L., Yang, K.R., Motapothula, M.R., Ren, D., Lobaccaro, P., Patra, A., Sherburne, M., Batista, V.S., Yeo, B.S., Ager, J.W., et al. (2018). Investigating the role of copper oxide in electrochemical CO2 reduction in real time. ACS Appl. Mater. Interfaces 10, 8574–8584. https://doi.org/10.1021/acsami.7b15418.

125. Ren, D., Deng, Y., Handoko, A.D., Chen, C.S., Malkhandi, S., and Yeo, B.S. (2015). Selective electrochemical reduction of carbon dioxide to ethylene and ethanol on copper (I) oxide catalysts. ACS Catal 5, 2814–2821. https://doi.org/10.1021/cs502128q.

126. Löffler, M., Mayrhofer, K.J.J., and Katsounaros, I. (2021). Oxide reduction precedes carbon dioxide reduction on oxide-derived copper electrodes. J. Phys. Chem. C 125, 1833–1838. https://doi.org/10.1021/acs.jpcc.0c09107s.

127. Zhao, Y., Chang, X., Malkani, A.S., Yang, X., Thompson, L., Jiao, F., and Xu, B. (2020). Speciation of Cu surfaces during the

Please cite this article in press as: Casebolt et al., Pulse check: Potential opportunities in pulsed electrochemical CO_2 reduction, Joule (2021), https://doi.org/10.1016/j.joule.2021.05.014

electrochemical CO reduction reaction. J. Am. Chem. Soc. 142, 9735–9743. https://doi.org/10.1021/jacs.0c02354.

128. Chang, C.-J., Hung, S.-F., Hsu, C.-S., Chen, H.-C., Lin, S.-C., Liao, Y.-F., and Chen, H.M. (2019). Quantitatively unraveling the redox shuttle of spontaneous oxidation/electroreduction of CuOx on silver nanowires using in situ X-ray absorption spectroscopy. ACS Cent. Sci. 5, 1998–2009. https://doi.org/10.1021/acscentsci.9b01142.

129. Todorova, T.K., Schreiber, M.W., and Fontecave, M. (2020). Mechanistic understanding of CO 2 reduction reaction (CO2RR) toward multicarbon products by heterogeneous copper-based catalysts. ACS Catal 10, 1754–1768. https://doi.org/10.1021/acscatal.9b04746.

130. Li, C.W., Ciston, J., and Kanan, M.W. (2014). Electroreduction of carbon monoxide to liquid fuel on oxide-derived nanocrystalline copper. Nature 508, 504–507. https://doi.org/10.1038/nature13249.

131. Feng, X., Jiang, K., Fan, S., and Kanan, M.W. (2016). A direct grain-boundary-activity correlation for CO electroreduction on Cu nanoparticles. ACS Cent. Sci. 2, 169–174. https://doi.org/10.1021/acscentsci.6b00022.

132. Wang, L., Nitopi, S., Wong, A.B., Snider, J.L., Nielander, A.C., Morales-Guio, C.G., Orazov, M., Higgins, D.C., Hahn, C., and Jaramillo, T.F. (2019). Electrochemically converting carbon monoxide to liquid fuels by directing selectivity with electrode surface area. Nat. Catal. 2, 702–708. https://doi.org/10.1038/s41929-019-0301-z.

133. Lee, S., and Lee, J. (2018). Ethylene selectivity in CO electroreduction when using Cu oxides: an in situ ATR-SEIRAS study. ChemElectroChem 5, 558–564. https://doi.org/10.1002/celc.201700892.

134. Liu, X., Schlexer, P., Xiao, J., Ji, Y., Wang, L., Sandberg, R.B., Tang, M., Brown, K.S., Peng, H., Ringe, S., et al. (2019). pH effects on the electrochemical reduction of CO(2) towards C2 products on stepped copper. Nat. Commun. 10, 32. https://doi.org/10.1038/s41467-018-07970-9.

135. Liu, C., Hedström, S., Stenlid, J.H., and Pettersson, L.G.M. (2019). Amorphous, periodic model of a copper electrocatalyst with subsurface oxygen for enhanced CO coverage and dimerization. J. Phys. Chem. C 123, 4961–4968. https://doi.org/10.1021/acs.jpcc.8b12214.

136. Chen, X., Henckel, D.A., Nwabara, U.O., Li, Y., Frenkel, A.I., Fister, T.T., Kenis, P.J.A., and Gewirth, A.A. (2020). Controlling speciation during CO2 reduction on Cu-alloy electrodes. ACS Catal 10, 672–682. https://doi.org/10.1021/acscatal.9b04368.

137. Xiao, H., Goddard, W.A., Cheng, T., and Liu, Y. (2017). Cu metal embedded in oxidized matrix catalyst to promote CO2 activation and CO dimerization for electrochemical reduction of CO2. Proc. Natl. Acad. Sci. USA 114, 6685–6688. https://doi.org/10.1073/pnas.1702405114.

138. De Luna, P., Quintero-Bermudez, R., Dinh, C.-T., Ross, M.B., Bushuyev, O.S., Todorović, P., Regier, T., Kelley, S.O., Yang, P., and Sargent, E.H. (2018). Catalyst electro-redeposition controls morphology and oxidation state for selective carbon dioxide reduction. Nat. Catal. 1, 103–110. https://doi.org/10.1038/s41929-017-0018-9.

139. Sebastián-Pascual, P., and Escudero-Escribano, M.a. (2020). Addressing the interfacial properties for CO electroreduction on Cu with cyclic voltammetry. ACS Energy Lett 5, 130–135. https://doi.org/10.1021/acsenergylett.9b02456.

140. Simon, G.H., Kley, C.S., and Roldan Cuenya, B. (2021). Potential-dependent morphology of Copper catalysts during CO2 electroreduction revealed by in situ atomic force microscopy. Angew. Chem. Int. Ed. Engl. 60, 2561–2568. https://doi.org/10.1002/anie.202010449.

141. Kas, R., Kortlever, R., Yilmaz, H., Koper, M.T.M., and Mul, G. (2015). Manipulating the hydrocarbon selectivity of copper nanoparticles in CO2 electroreduction by process conditions. ChemElectroChem 2, 354–358. https://doi.org/10.1002/celc.201402373.

142. Kim, Y.G., Baricuatro, J.H., Javier, A., Gregoire, J.M., and Soriaga, M.P. (2014). The evolution of the polycrystalline copper surface, first to Cu(111) and then to Cu(100), at a fixed CO_2RR potential: a study by operando EC-STM. Langmuir 30, 15053–15056. https://doi.org/10.1021/la504445g.

143. Kim, Y.-G., Baricuatro, J.H., and Soriaga, M.P. (2018). Surface reconstruction of polycrystalline Cu electrodes in aqueous KHCO3 electrolyte at potentials in the early stages of CO2 reduction. Electrocatalysis 9, 526–530. https://doi.org/10.1007/s12678-018-0469-z.

144. Kim, Y.-G., Javier, A., Baricuatro, J.H., Torelli, D., Cummins, K.D., Tsang, C.F., Hemminger, J.C., and Soriaga, M.P. (2016). Surface reconstruction of pure-Cu single-crystal electrodes under CO-reduction potentials in alkaline solutions: A study by seriatim ECSTM-DEMS. J. Electroanal. Chem. 780, 290–295. https://doi.org/10.1016/j.jelechem.2016.09.029.

145. Schouten, K.J.P., PérezGallent, E., and Koper, M.T.M. (2013). Structure sensitivity of the electrochemical reduction of carbon monoxide on copper single crystals. ACS Catal 3, 1292–1295. https://doi.org/10.1021/cs4002404.

146. Sebastián-Pascual, P., Sarabia, F.J., Climent, V., Feliu, J.M., and Escudero-Escribano, M. (2020). Elucidating the structure of the Cu-alkaline electrochemical interface with the laser-induced temperature jump method. J. Phys. Chem. C 124, 23253–23259. https://doi.org/10.1021/acs.jpcc.0c07821.

147. Hori, Y., Takahashi, I., Koga, O., and Hoshi, N. (2003). Electrochemical reduction of carbon dioxide at various series of copper single crystal electrodes. Journal of Molecular Catalysis A: Chemical 199, 39–47. https://doi.org/10.1016/S1381-1169(03)00016-5.

148. De Gregorio, G.L., Burdyny, T., Loiudice, A., Iyengar, P., Smith, W.A., and Buonsanti, R. (2020). Facet-dependent selectivity of Cu catalysts in electrochemical CO2 reduction at commercially viable current densities. ACS Catal 10, 4854–4862. https://doi.org/10.1021/acscatal.0c00297.

149. Jung, H., Lee, S.Y., Lee, C.W., Cho, M.K., Won, D.H., Kim, C., Oh, H.S., Min, B.K., and Hwang, Y.J. (2019). Electrochemical fragmentation of Cu2O nanoparticles enhancing selective C–C coupling from CO2 reduction reaction. J. Am. Chem. Soc. 141, 4624–4633. https://doi.org/10.1021/jacs.8b11237.

150. Schouten, P., P., K.J., Gallent, E.P., and Koper, M.T.M. (2013). The electrochemical characterization of copper single-crystal electrodes in alkaline media. J. Electroanal. Chem. 699, 6–9. https://doi.org/10.1016/j.jelechem.2013.03.018.

151. Bunea, S., and Urakawa, A. (2021). In situ spectroscopic methods to study electrochemical CO2 reduction. In Carbon Dioxide Electrochemistry: Homogeneous and Heterogeneous Catalysis, C.C. Marc Robert and K. Daasbjerg, eds. (The Royal Society of Chemistry), pp. 347–407.

152. Malkani, A.S., Anibal, J., Chang, X., and Xu, B. (2020). Bridging the gap in the mechanistic understanding of electrocatalysis via in situ characterizations. iScience 23, 101776. https://doi.org/10.1016/j.isci.2020.101776.

153. Handoko, A.D., Wei, F., Jenndy, Yeo, B.S., and Seh, Z.W. (2018). Understanding heterogeneous electrocatalytic carbon dioxide reduction through operando techniques. Nat. Catal. 1, 922–934. https://doi.org/10.1038/s41929-018-0182-6.

154. Clark, E.L., Resasco, J., Landers, A., Lin, J., Chung, L.-T., Walton, A., Hahn, C., Jaramillo, T.F., and Bell, A.T. (2018). Standards and protocols for data acquisition and reporting for studies of the electrochemical reduction of carbon dioxide. ACS Catal 8, 6560–6570. https://doi.org/10.1021/acscatal.8b01340.

155. Singh, M.R., Clark, E.L., and Bell, A.T. (2015). Effects of electrolyte, catalyst, and membrane composition and operating conditions on the performance of solar-driven electrochemical reduction of carbon dioxide. Phys. Chem. Chem. Phys. 17, 18924–18936. https://doi.org/10.1039/C5CP03283K.

156. Rabiee, H., Ge, L., Zhang, X., Hu, S., Li, M., and Yuan, Z. (2021). Gas diffusion electrodes (GDEs) for electrochemical reduction of carbon dioxide, carbon monoxide, and dinitrogen to value-added products: a review. Energy Environ. Sci. 14, 1959–2008. https://doi.org/10.1039/D0EE03756G.